



**NTNU – Trondheim**  
Norwegian University of  
Science and Technology

# Formation Evaluation and Uncertainty Analysis of the Ormen Lange Field, Norwegian Sea offshore Norway

**Maura Patricia Segunda**  
**Gimbe**

Petroleum Geosciences

Submission date: June 2015

Supervisor: Stephen John Lippard, IGB

Norwegian University of Science and Technology  
Department of Geology and Mineral Resources Engineering



**Norwegian University of Science and Technology**  
**Department of Petroleum Engineering and Applied Geophysics**

**MSC PROJECT IN PETROLEUM GEOSCIENCE**

**Formation Evaluation and Uncertainty Analysis of the Ormen Lange Field, Norwegian Sea  
offshore Norway**

By

Maura Patricia Segunda Gimbe

**Supervisor:** Stephen John Lippard

## **PREFACE**

This report is a part of the fulfillment for the degree of Master of Science in Petroleum Geosciences at the Norwegian University of Science and Technology (NTNU). The information present in this report is based on literature research, petrophysical analysis and uncertainty estimation of reservoir properties. The work was performed by using Techlog software from Schlumberger.

## ABSTRACT

Formation evaluation is the process of analyzing and interpreting geophysical data performed as a function of wellbore depth, by describing the processes that determine the viability of a formation to produce hydrocarbons. According to the data availability, formation evaluation can be done using core data, well log and initial production data.

The aim of this study was to do the formation evaluation using petrophysical parameters from wireline logs in order to determine lithology, porosity, permeability and fluid saturation and to understand the importance of the uncertainty analysis on reservoir permeability and predict gas recovery.

In this work, Techlog software was used to perform a robust computation of petrophysical properties and then give summaries computed petrophysical properties. A formation evaluation module is a set of solutions for conventional log interpretation. In the summaries module the computed average of shale volume, porosity and water saturation are used to determine the reservoir interval pay zone. The permeability computation uncertainty analysis presented in this paper was done by using Monte-Carlo simulation that allowed understanding the relative weight of each variable by analyzing the sensitive case interpreting the tornado plot result. The gas recovery was predicted based on porosity, saturation and net productive thickness average of all the given wells.

It is important to identify properly the lithology and the reservoir to allow an accurate petrophysical calculation of porosity, water saturation and permeability.

The determination of lithology based on cross-plot neutron versus density log was important step to come up with the reservoir petrophysical properties. The quality of the reservoir as determined by permeability is good with permeability value around 45, 135 mD and by porosity was very good values between 24 to 30 percent.

In general by plotting porosity values against permeability values showed strong linear relationship between the two variables of the reservoir indicating that Ormen Lange field reservoir are permeable. It should be noted that the presence of shale in the entire reservoir influenced negatively in the permeability values. The petrophysical properties of the reservoir in Ormen Lange field are enough to permit hydrocarbon production.

Keywords: Formation evaluation; Sandstone; Petrophysical properties; Reservoir property; Ormen Lange field; Uncertainty analyses.

## **ACKNOWLEDGEMENT**

I would like to thank God as the Creator of the world for all his help during the elaboration of this work and for keeping me alive and giving me the strength in the presence of weakness.

My sincerest and greatest thanks goes to the persons that have strongly been involved in this work; Professor Stephen John Lippard, academic supervisor and Yahaya Mohamed, company supervisor for their guidance and well-proven experience.

Likewise, I would like to thank Statoil and the Norwegian University of Science and Technology (NTNU) for this opportunity and its professors such as Egil Tjaland, Jon kleppe and Mai Britt E. Mørk for help during my studies. To all SIS Angola team in Schlumberger company for their support and friendless during my internship with them.

Finally, I would also like to thank my family, especially my mother Guilhermina Segunda Gimbe, Father Jacinto Gimbe, my husband Armindo Bango, my sisters Elsa Catarina, Hermenegilda Gilda, Ruth Marlene, Luisa Daniela and my brothers Rosario Antonio and Helder Manuel for all the advice and motivation. The members of the ANTHEI group, in particular, the most recent members of the group (ANTHEI 2012) especially Diawako Garcia for their skilled, social and spiritual support.

## CONTENT

PREFACE	I
ABSTRACT	II
ACKNOWLEDGEMENT	III
List of Figures	VI
List of Tables	VII
Nomenclature	VIII
CHAPTER 1 – INTRODUCTION	1
1.1 Project outline	2
1.2 - Objective	2
CHAPTER 2 - FIELD DESCRIPTION	3
2.1 Ormen Lange Field	3
2.2 – Geological information	5
2.3- Lithostratigraphy of the reservoir interval	6
2.4 -Depositional model and facies characterization	8
CHAPTER 3- BACKGROUND THEORY	11
3.1 Main petrophysical properties	11
3.1.1 Porosity	11
3.1.2 Porosity type	12
3.1.3 Porosity determination	13
3.2. Permeability	13
3.2.1 Factors effecting permeability	14
3.3 Fluids Saturation	16
3.3 Hydrocarbon volume calculation	18
3.4 Uncertainty Estimation	19
3.4.1 Monte Carlo simulation	20
CHAPTER 4- METHODOLOGY	22
4.1 Provided data	22
4.2 Data loading and quality control	22

4.3 - Workflow implemented to perform the formation evaluation using Techlog .....	23
4.4 Pre computation workflow -----	24
4.4.1 Bad hole flag -----	24
4.4.2 Borehole computation-----	26
4.5 Petrophysical properties computation .....	26
4.5.1 Lithology Determination -----	27
4.5.2 Shale Volume Computation -----	28
4.5.3 Total Porosity and Saturation from Neutron- Density -----	29
4.5.4 Effective Porosity from Neutron-Density -----	30
4.5.5 Permeability computation -----	32
4.5.6 Summaries-----	33
CHAPTER 5- ANALYSIS AND RESULTS -----	34
5.1 Lithology Determination .....	34
5.2 Zonation .....	43
5.3 Vertical and lateral Variability .....	51
5.4 Pre-computation .....	52
5.5 Petrophysical Properties computation .....	52
5.6 Permeability uncertainty analysis .....	58
5.7 Porosity and permeability relationship on reservoir Zone.....	61
5.7 Hydrocarbon volume Calculation .....	62
CHAPTER 6- DISCUSSION -----	64
CHAPTER 7- CONCLUSION -----	65
REFERENCES -----	66

## List of Figures

Figure 1: Ormen Lang field location map (Möller, 2004)-----	4
Figure 2: Figure 3: Location map with the main Jurassic-Cretaceous structural elements. Modified from Dore and Lundin (1996) -----	6
Figure 3: Ormen Lange Reservoir sandstone of different age (Moller, 2004) -----	8
Figure 4: Comparative reservoir architecture of deep water channel. (Sprague et al., 2005) -----	10
Figure 5: Definition of Darcy law. (Darcy 1950). -----	14
Figure 6: Textural parameter and permeability (Link, 1982)-----	15
Figure 7: Tornado Plot illustration (Techlog 2013.4)-----	21
Figure 8: Neutron-density cross-plot (Techlog 2013.4) -----	28
Figure 9: Cross plot Neutron Porosity vs Bulk Density (TNPH) for well 6305_4-1(Techlog 2013.4) -----	34
Figure 10: Cross plot Neutron Porosity vs Bulk Density (TNPH) for well 6305_4-1(Techlog 2013.4) -----	35
Figure 11: Cross plot Neutron Porosity vs Bulk Density for well 6305_4-2S (Techlog 2013.4) -----	36
Figure 12: Cross plot Neutron Porosity vs Bulk Density (TNPH) for well 6305_4-2S (Techlog 2013.4)----	37
Figure 13: Cross plot Neutron Porosity vs Bulk Density (TNPH) for well 6305_5-1 (Techlog 2013.4)-----	38
Figure 14: : Cross plot Neutron Porosity vs Bulk Density (TNPH) for well 6305_5-1 (Techlog 2013.4)----	39
Figure 15: : Cross-plot, Neutron Porosity vs Bulk Density (TNPH) for well 6305_7-1 (Techlog 2013.4)---	40
Figure 16: Cross plot Neutron Porosity vs Bulk Density (TNPH) for well 6305_5-1 (Techlog 2013.4)-----	41
Figure 17: : Cross-plot, Neutron Porosity vs Bulk Density (TNPH) for well 6305_8-1 (Techlog 2013.4)---	42
Figure 18: Cross-plot, Neutron Porosity vs Bulk Density (TNPH) for well 6305_8-1 (Techlog 2013.4)-----	43
Figure 19: Well zone description for well 6305_4-1-----	45
Figure 20: Well zone description for well 6305_4-2S-----	46
Figure 21: Well zone description for well 6305_5-1-----	48
Figure 22: Well zone description for well 6305_7-1-----	49
Figure 23: Well zone description for well 6305_8-1-----	50
Figure 24: Well correlation for the 5 given wells at reservoir level -----	51
Figure 25: Petrophysical properties for well 6305_4-1 -----	53
Figure 26: Petrophysical properties for well 6305_4-2S -----	54
Figure 27: Petrophysical properties for well 6305_5-1 -----	55
Figure 28: Petrophysical properties for well 6305_7-1 -----	56
Figure 29: Petrophysical properties for well 6305_8-1 -----	57
Figure 30: Sensitivity analysis for well 6305_4-1 -----	58
Figure 31: Sensitivity analysis for well 6305_4-2S -----	59
Figure 32: Sensitivity analysis for well 6305_5-1 -----	59
Figure 33: Sensitivity analysis for well 6305_7-1 -----	60
Figure 34: Sensitivity analysis for well 6305_8-1 -----	60
Figure 35: Cross plot Multi-well (PHIE vs PERM Coates)-----	61

## List of Tables

Table 1 – Respective percentage of company’s shares -----	4
Table 2 Porosity type-----	13
Table 3 - Reservoir permeability classification (modified after Glover, 2011)-----	15
Table 4 - Standard units used in oil industry-----	19
Table 5 - Input Parameters of the bad hole computation -----	24
Table 6 - Bad hole computation with specific zonation interval -----	24
Table 7 - Bad hole computation parameter set up -----	25
Table 8 - Borehole computation input -----	26
Table 9 - Input variable for total porosity and saturation-----	30
Table 10 - Input Variable for Effective porosity and saturation computation -----	32
Table 11- Permeability input parameter-----	33
Table 12 - Reservoir flag Cutoff -----	33

## Nomenclature

$m^3$ : Cubic meters

$\Phi$  : Porosity

A : Area of zone

API: American Petroleum Institute

FGOR: Field Gas Oil Ratio

GOIP: Gas initially in place

GOR: Gas Oil Ratio

$h$ : Thickness

mD: Mille Darcy

MD: Measure depth

OIIP: Oil Initially In Place

STGOIP: Stock tank gas originally in place

STOOIP: Stock tank oil originally in place

SW: Water saturation

TVD: True Vertical Depth

OWC: Oil Water Contact

OWT: One way time

WH: Well head

## CHAPTER 1 – INTRODUCTION

Lithological layers location and properties determination needs acquisition and interpretation of well logs. Once cuttings are pumped out to surface, a log can be drawn by hand to reflect lithology, and in others cases they can be acquired by wireline logging tools lowered into the well or coring. After that, interpretation can be carried out by hand, using established log analysis formulae, or by computer using appropriate software.

Nowadays in the petroleum industry, formation evaluation is being used for many reasons, such as a base to understand the geology of the wellbore at high resolution and also to estimate the producible hydrocarbon reservoir. One of the most useful ways to perform a formation evaluation is by use of well logs, because they can contain key information about the formation sampled by different petrophysical measurements (William, et al., 2011).

Formation evaluation is still a challenge in many fields because of the complexity of the reservoir environment subsequent diagenesis effect. Therefore, the identification and understanding of such phenomena is important before any well evaluation. In recent years, newly developed technology and software and considerable work has been done in order to deal with this issue and minimize the uncertainties associated with the hydrocarbon presence perform the economic evaluation.

Once formation evaluation is performed on the reservoir, it is crucial to pay attention to the location of the possible reservoir zone in the drilled section, determination of fluid type (gas, oil, water) present in the pore space, saturation level, and the mobility of the fluids across the connected pore space of the rock. To better achieve such information it is important to have a good understanding of porosity (total, primary, effective porosity), water saturation computation, pay thickness and selection of cutoffs. The aim of this process is to economically establish the existence of producible reservoirs. For that reason some aspects such as uncertainty analysis in reservoir properties measurement are needed in order to understand and quantify potential risks, that could impact in our hydrocarbon presence and consequently in wrong decisions being made (Adams, 2005).

Techlog software, as a wellbore platform, can deal with both basic and advanced formation evaluation and uncertainty analyses on all wellbore data types available. This allow the possibility to design your own petrophysical workflow to generate significant quick look interpretations based on your knowledge, and brings all of your wellbore data on vastly intuitive application to carry out analyses.

In this present work Techlog performed formation evaluation using well data in order to determine the petrophysical properties and predict the hydrocarbon presence in the reservoir of the Ormen Lange gas field in the Norwegian sea, Offshore Norway.

## 1.1 Project outline

This project will be carried out using Schlumberger`s Techlog software, where the well logs data are loaded into the program in order to perform the formation evaluation. In the early stage petrophysical analysis and Monte-Carlo simulation are done to estimate uncertainty on reservoir permeability and in the final stage gas prediction recovery is done.

This study is structured in the following way: Chapter 2 - Field description, which describes the geological setting of the field. Chapter 3 - Background theory, where the main theory regarding the topic is presented. Chapter 4 - Methodology, which describes in detail the formation evaluation steps, developed using Techlog. Chapter 5 - Analysis and results, which presents tables, figures, logs, and arguing the findings and, finally, Chapter 6 Conclusion, which covers the main aspects of the work.

## 1.2 - Objective

The objectives in this work are summarized as follows:

- ❖ Lithology determination using cross-plots
- ❖ Porosity, permeability, fluids saturation determination in the reservoir zone
- ❖ Understanding the importance of the uncertainty analysis on reservoir permeability
- ❖ Prediction of gas recovery

## CHAPTER 2 - FIELD DESCRIPTION

### 2.1 Ormen Lange Field

Ormen Lange is a gas field located in the Møre Basin in the southern part of the Norwegian Sea in the Norwegian continental shelf (Figure 1). It is operated by Norsk Hydro and Norske Shell in the development and production phases respectively. Other partners like Statoil, Shell, Petoro, Dong and Exxon Mobil have their respective percentage of shares (Table 1). Discovered in 1997 the field is located approximately 125 km offshore Norway north-west of Kristiansund, the sea depth in the area is about 700 to 1,100 meters and areal extent of the field is about 350 km (Moller, 2004). The reservoir is approximately 40 kilometers long and 8 kilometers wide, and lies about 3,000 meters below sea level. Production began in September 2007 and it is the second largest gas field in Norway with recoverable gas reserves estimated at 397 billion Sm<sup>3</sup> gas in place (GIIP) and 28.5 million Sm<sup>3</sup> of condensate. During the appraisal and exploration phase five wells were drilled, but only four of them showed the presence of gas and there was one dry well (Eirik et al., 2004). The gas is dry (GCR of approximately 11,000 Sm<sup>3</sup>/Sm<sup>3</sup>). The main reservoir consists of sandstones of Paleocene age in the "Egga" Formation, about 2700 - 2900 meters below sea level. The porosity of the reservoir is about 24-32%, and the reservoir is faulted by non-tectonic faults related to sediment compaction and fluid expulsion.



Figure 1: Ormen Lang field location map (Möller, 2004)

Table 1 – Respective percentage of company’s shares

Company name	Share (%)
Statoil	10.8
Dong	10.3
Exxonmobil	7.2
Shell	17.0
Norsk Hydro	18.1
Petoro	36.5

## 2.2 – Geological information

The Ormen Lange field is represented by a turbidite system reservoir developed in Late Cretaceous (Maastrichtian) and Early Paleocene (Danian) times, prior to the early Eocene onset of seafloor spreading in the Norwegian-Greenland Sea. The base Tertiary surface is evidently conformable within the area of the field, although there is biostratigraphic evidence for a stratigraphic break within the underlying Upper Maastrichtian (Doré et al., 1996).

An approximately Base Tertiary unconformity is developed in the adjacent Slørebotn Basin to the south and the Frøya High to the east. The turbidity system lies basin ward of two converging fault zones, the first comprising the Møre–Trøndelag Fault Complex and associated Gossa High, trending NE–SW, and the second being the Klakk Fault Complex, trending close to N–S. The main gas reserves lie in a reservoir in the Vale formation (Möller et al., 2004).

The reservoir represents an extensive coastal spit system with sedimentary input from the different turbidity sequence. The coastal and shallow marine sediment supply system is not preserved because of the erosional processes that happened during the uplift of the Norwegian mainland (Riis, 1996).

The Ormen Lange field has a structural configuration of a dome as shown in figure 2, revealing a structural closure (Doré et al., 1996).

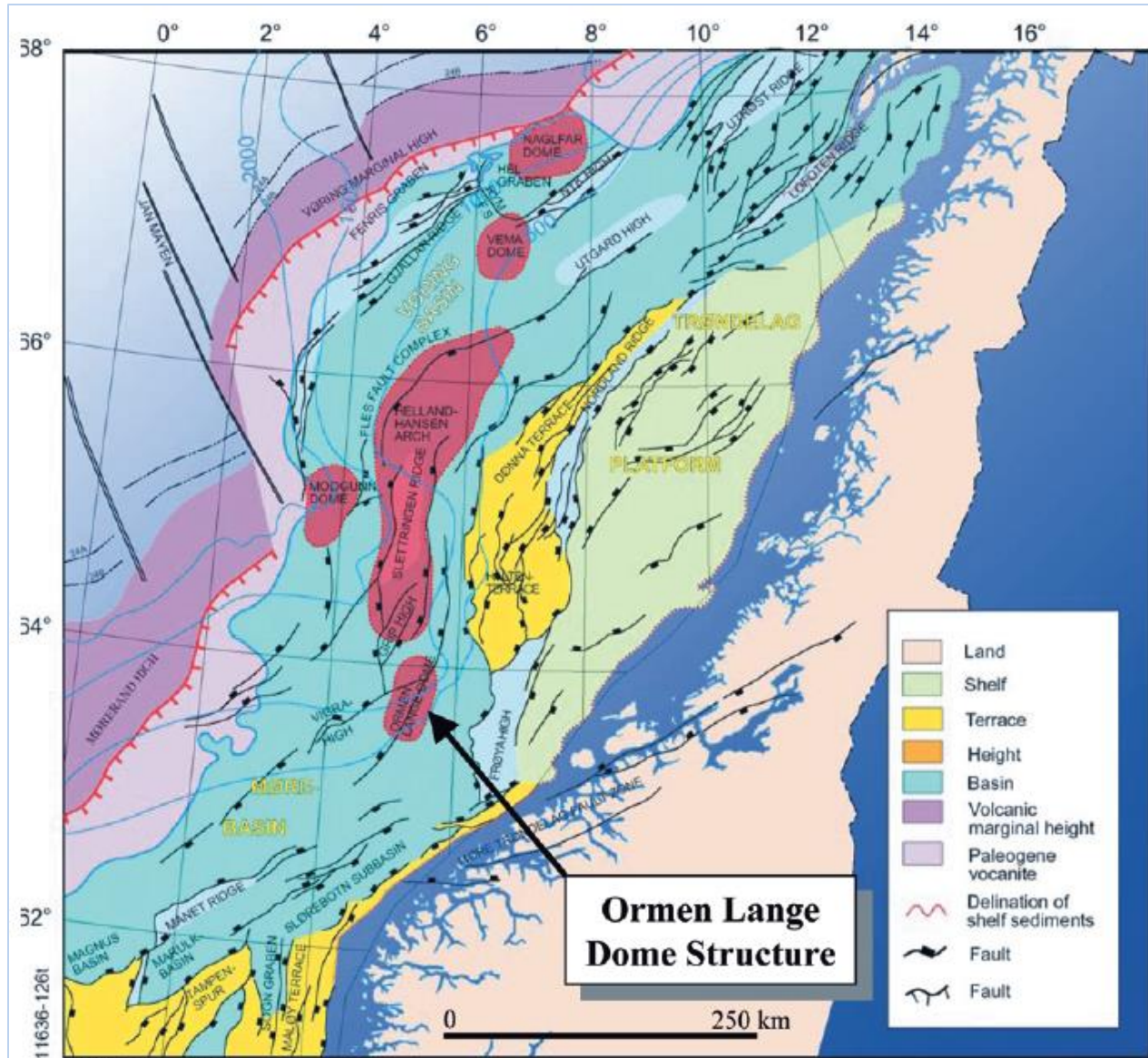


Figure 2: Figure 3: Location map with the main Jurassic-Cretaceous structural elements. Modified from Dore and Lundin (1996)

### 2.3- Lithostratigraphy of the reservoir interval

The reservoir interval is from Late Cretaceous (Maastrichtian) to Early Tertiary (Early Paleocene) age as shown in Figure.3. The Egga Sandstone Member (Danian), that is represented by Vale formation which represents the main reservoir interval, has been subdivided into three reservoir zones: The Egga Reservoir unit (Egga RU), which comprises the massive part of the Egga Member, the "Våle Tight", extensive intra reservoir shale, and the Våle Heterolithic unit, which is characterized by sand/shale alternations (Möller et al., 2004).

The Late Cretaceous ( Maastrichtian ) part of the reservoir is represented by the Jorsalfare Formation, that consists of sandstone, mudstone and limestone alternations with a slight increase in sand content upwards, accompanied by a thickening upwards of individual sandstone beds. This variation was well noticed in the well log analyzed in Chapter 4, where well 6305/7-2 contains a significantly higher sand content than other wells. The upper and lower part of the Maastrichtian deposits show a similar facies development, but with the main difference being that they are individual turbidities are thicker with thinner mudstone intervals between each turbidite..

There is also in the lower part of the succession a preponderance of high density turbidities and there are interbedded with strongly bioturbated mudstones and some bioturbated chalk in the middle part of the interval. This evidence is a good indicator of a period of low siliciclastic accumulation, helped by climatic conditions created at that time, which allowed the preservation of some carbonate particles as a cement close to the sea floor. This is a particularly characteristic in the Maastrichtian sand in contrast with the Tertiary sands, which only display minor carbonate cementation (Möller et al., 2004).

Furthermore, the stratigraphic development of the Cretaceous reservoir section suggests a depositional environment dominated by slow background sedimentation from suspension fall out in a fairly well-oxygenated, open marine basin. This was interrupted by pulses of deposition from turbidity currents.

In the Tertiary (Paleocene) the reservoir is represented by the Våle Formation that is sand dominated toward the top of the formation and represents the main reservoir interval. The Egga Member is dominated by turbidity sandstones of massive amalgamated or weakly separated sands that have good reservoir properties due to their poor lithification, well seen in the lower part.

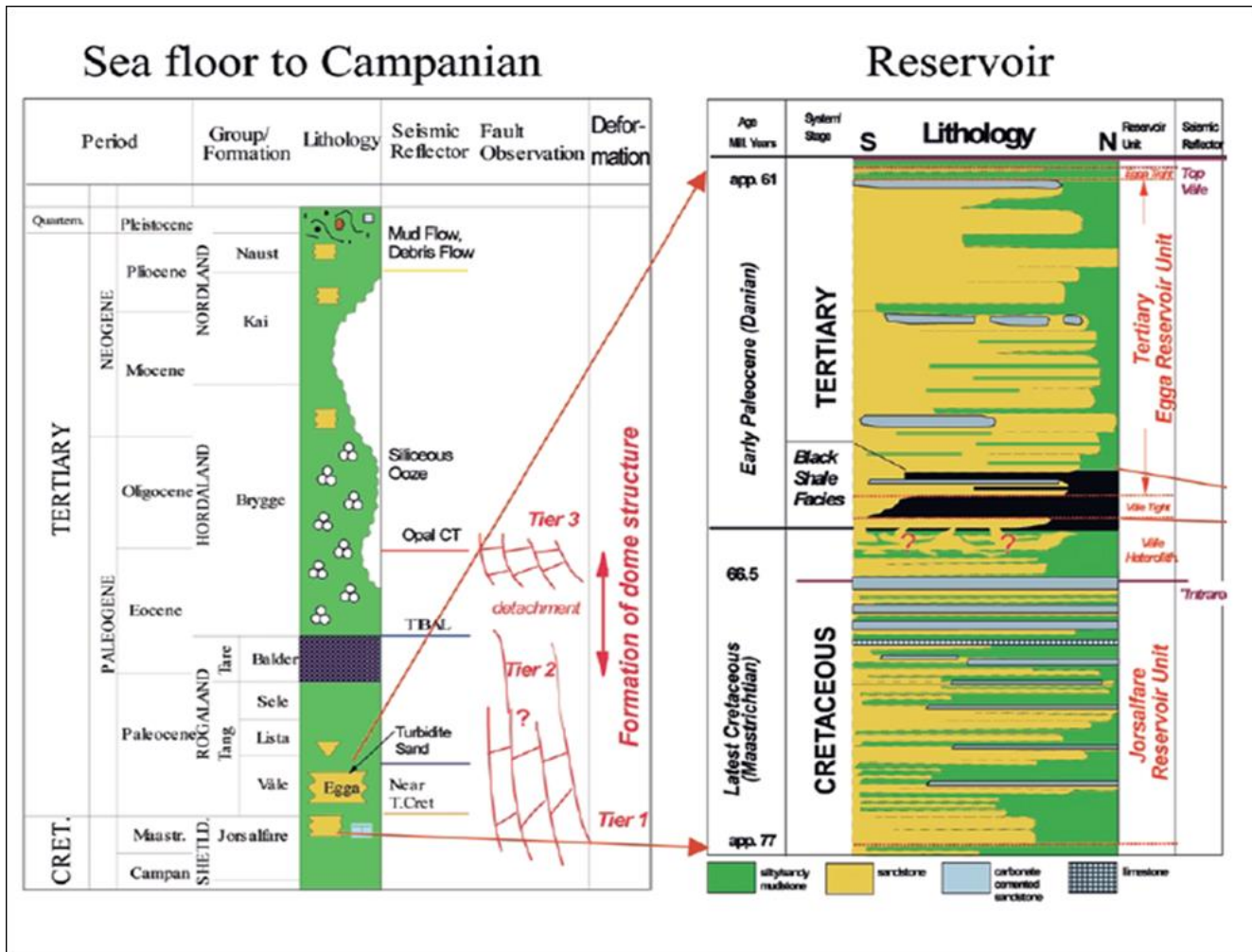


Figure 3: Ormen Lange Reservoir sandstone of different age (Moller, 2004)

## 2.4 -Depositional model and facies characterization

The Ormen Lange turbidites are thought to be derived from slumping in the tectonically unstable ramp area between the Klakk and Møre-Trøndelag fault systems. Subarkosic sandstones with a fine-grained sand modal grain size provide the reservoir and coarse tails range up to granule grade in some instance showing evidence of high to low concentration turbidite (Figure.4).

According to Moller et al., (2004), most of the reservoir units of Paleocene age in this field were deposited by high- density turbidity currents in a N-S elongated, structurally controlled sub-basin.

The basin is described as a narrowing considerably towards the north and the basin floor is tilted slightly towards the east. Deposition was confined by topography, preferentially preserving the coarsest grained deposits of the most powerful suspension currents (Möller et al., 2004).

Basin topography was continuously rejuvenated by differential subsidence along propagating polygonal faults due to the differential compaction of underlying Cretaceous shales and fault planes are frequent and are characterized by strongly varying throws.

As illustrated in figure.4, according to Sprague et al., (2005), low concentration turbidity beds are often associated with channel margin, levee and overbank deposition and as such, have good lateral continuity, whereas the vertical connectivity is commonly poor. This is because they tend to be thin bedded and are interbedded with shale, whereas high concentration turbidite beds are typically in channel deposits, and are characterized by amalgamation in axial positions (Sprague et al., 2005). They have good channel continuity and vertical connectivity. In this situation there are sand beds with more uniform reservoir quality, mounded geometry, and restricted distribution. Reservoir connectivity is determined by the number of mounds and their degree of amalgamation (Shepherd., 2009).

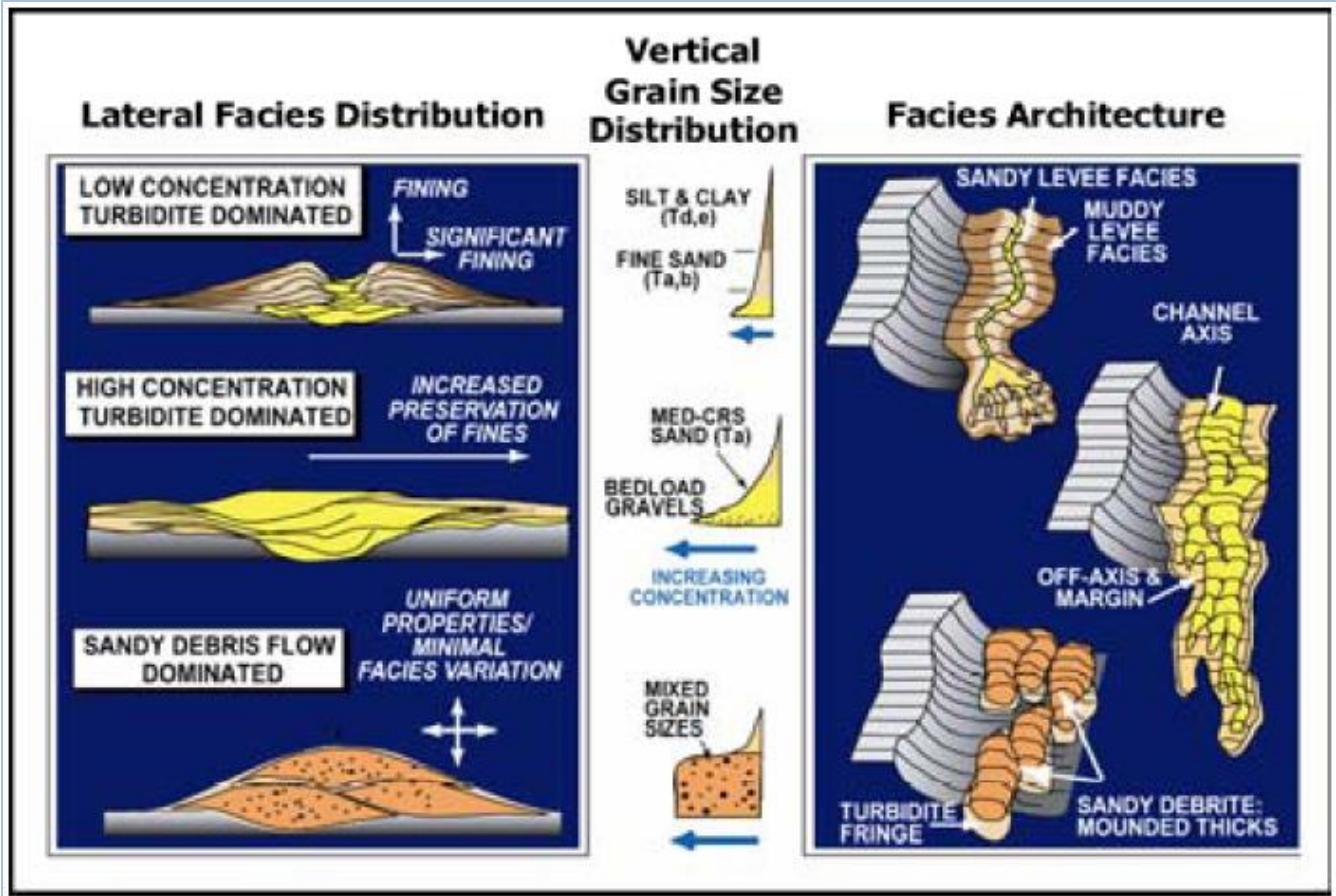


Figure 4: Comparative reservoir architecture of deep water channel. (Sprague et al., 2005)

## CHAPTER 3- BACKGROUND THEORY

This chapter will outline the concepts related to formation evaluation and uncertainty analysis. It will illustrate and discuss the following petrophysical properties: porosity, permeability and water saturation. The uncertainty analysis will focus solely on permeability as it is considered to be the main petrophysical property from the exploration to production phase of hydrocarbons (Theodoor, 2000)

### 3.1 Main petrophysical properties

The determination of petrophysical properties in the oil industry is very important, seeing that they help to know the economic viability of the reservoir (Wilson et al., 2004).

#### 3.1.1 Porosity

It is essential that the rock contains porous space, to allow the hydrocarbons to be stored. According to Dullien (1979), porosity is defined using the following statements:

The medium must contain spaces, or voids embedded in a solid matrix.

The medium must be permeable to liquid or gas which requires that the pores to be connected into the system.

Porosity is the key parameter in petrophysical evaluation, because of allowing the amount of hydrocarbons to be stored in the porous space of the rock (Theodoor, 2000).

Porosity can be calculated using the following mathematical relationship (equation 3.1)

$$\phi = \frac{V_{pore}}{V_{bulk}} = \frac{V_{bulk} - V_{rock}}{V_{bulk}} = \frac{V_{bulk} - (W/\rho_{rock})}{V_{bulk}} \quad (3.1)$$

Where:  $V_{pore}$  and  $V_{rock}$  are the volume of the pores and the rock respectively

$V_{bulk}$  = the bulk volume

$w$  = weight and  $\rho_{rock}$  is the specific density of the rock.

### 3.1.2 Porosity type

A number of different types of porosities are recognized and used within the hydrocarbon industry. The main ones are the total porosity and effective porosity. Related to the formation time they can also be classified as primary porosity, or secondary porosity (Table 2)

**Total porosity** is defined as the fraction of bulk volume of the reservoir rock that is occupied by fluid (Theodoor, 2000)

**Effective porosity** is defined as the total porosity minus the clay bound water (*equation 3.2*) by definition this effective porosity must be less than the total porosity.

$$\phi_c = \phi_T - \text{CBW} \quad (3.2)$$

Where :  $\phi_T$  is Porosity total

CBW = water bounded in clay that can not be removed.

**Primary porosity** is the initial porosity when the sediment was deposited. This can be classified as intergranular or intragranular

**Secondary porosity** results from the different phenomena such as diagenesis, compaction, bioturbation, clay coating and leaching which occur over geological time. This can be classified as intercrystalline, feneral, vuggy and fracture types (Storvoll, 2002).

Table 2 Porosity type

TIME OF FORMATION	TYPE	ORIGIN
During deposition (primary)	Intergranular	Sedimentation
	Intragranular	
After deposition (secondary)	Intercrystalline	Cementation
	Fenestral	
	Vuggy	Solution
	Moldic	
Fracture	Tectonics	

### 3.1.3 Porosity determination

Porosity can be either measured directly (neutron porosity) or calculated from variety of well logs (density, sonic, neutron, NMR). Those carried out by experiments on core extracted from the well are the most accurate. A combination of core and borehole porosity is used to optimize the accuracy of porosity results. Porosity using logs can be done stand-alone porosity tools (density, neutron, sonic, NMR) or combination tools (cross plot techniques).

According to Glover (2011), there are four most used methods of measuring porosity of cores: buoyancy, helium porosimetry, fluid saturation and mercury porosimetry. It is important to consider the inclusion and or exclusion of clay bound water volume while dealing with the different porosity measurement methods and treat it in different ways (Bilgesu et al., 1993).

### 3.2. Permeability

The ability of a porous medium to let the fluid to flow through is the permeability. For that to be possible a pore space of the rock must be connected by pathways. Permeability is important

because it is a rock property that relates to the rate at which hydrocarbons can be recovered (Darcy 1950).

Darcy's law is used expansively in petroleum engineering to determine flow through permeable media. The unit of measurement for permeability is the darcy, where  $1 \text{ D} = 0.9869 \times 10^{-12} \text{ m}^2$ . According to Glover (2011), one darcy is the permeability of a unit volume of sand at a pressure difference of 1 dyne/cm<sup>2</sup> between the ends of the sample that causes a fluid with a dynamic viscosity of 1 poise to flow a rate of 1 cm<sup>3</sup>/s (Figure 5).

$$Q = k \frac{A_t \Delta p}{\mu L} \quad (3.3)$$

Where  $Q$  = volumetric flow rate in m<sup>3</sup>/s through the porous medium with a total cross-section area  $A_t$  perpendicular to the flow direction

$\mu$  = dynamic viscosity of the fluid

$\Delta p$  = pressure drop across the porous medium with length  $L$

$k$  = the permeability

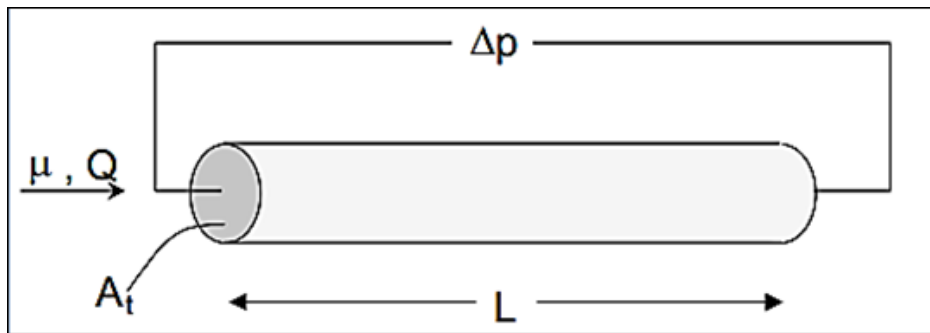


Figure 5: Definition of Darcy law. (Darcy 1950).

### 3.2.1 Factors effecting permeability

Formation permeability will be influenced by the following factors: pore size, grain size distribution, shape of grains, packing of grains. Figure 6, illustrates how permeability is affected by packing and sorting, the large rounded grains will have exceptional horizontal and vertical permeability. Very small angular grains will have very high horizontal permeability and fair vertical permeability.

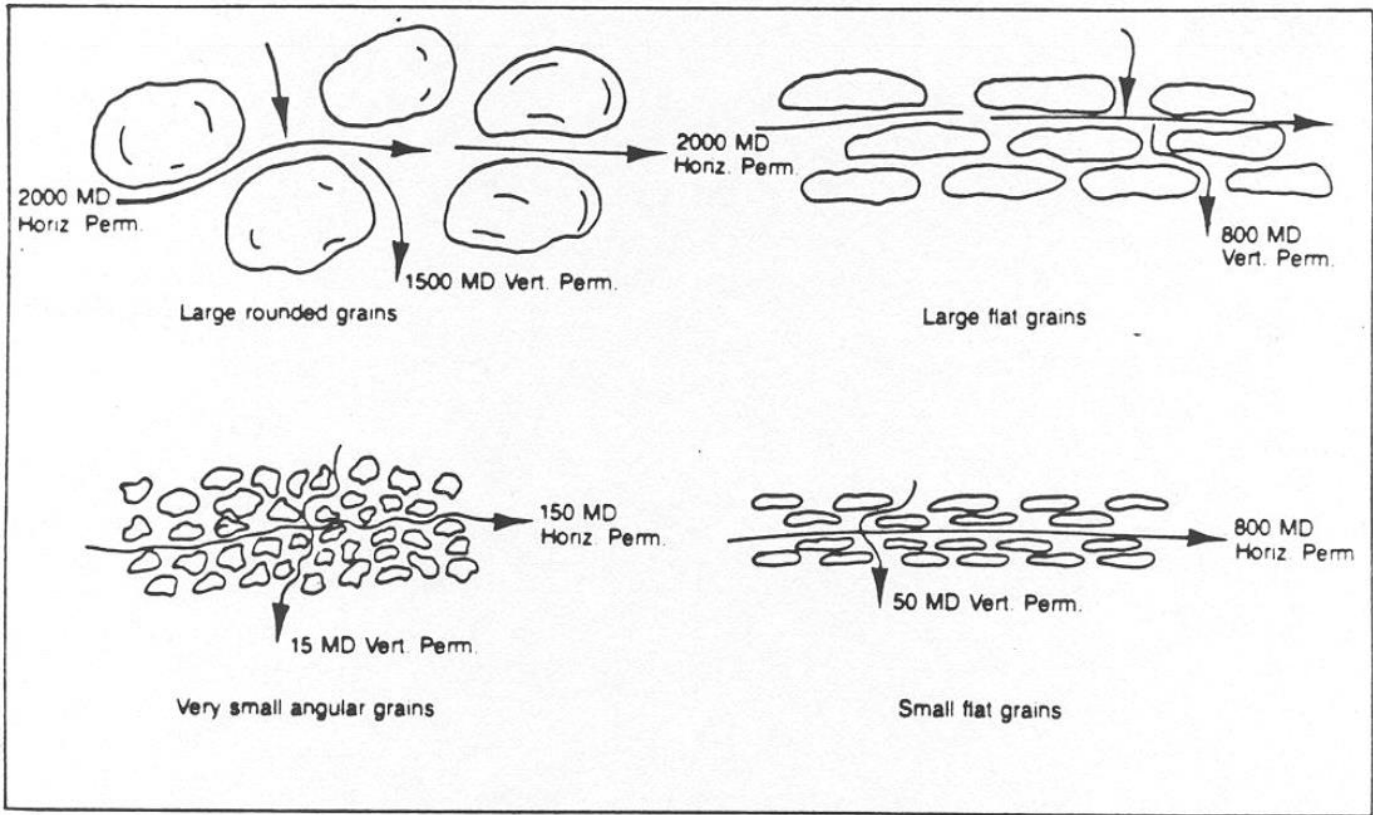


Figure 6: Textural parameter and permeability (Link, 1982)

### Permeability classification

Table 3 - Reservoir permeability classification (modified after Glover, 2011)

Permeability value (mD)	Classification
<10	Fair
10-100	High
100-1000	Very high
>1000	Exceptional

### 3.2.3 Permeability type

Permeability can be classified as absolute, effective and relative permeability.

Absolute permeability is the measure of the conductance of a porous media saturated with a single phase ( $s_w=1$ ).

Effective permeability is the conductance of a porous medium for one fluid phase when the media is saturated with more than two phases.

Relative permeability is the ratio of effective permeability of the oil, gas or water to the absolute permeability. Relative permeability can be expressed as a number between 0 and 1.0 or as percent.

### Permeability determination

Permeability can be derived from well logs, cores and/or well testing. In most case, cores and well test data are not available. Hence, the evaluation of permeability distribution from well log data in heterogeneous formations has technical importance as well economic advantage. However, it is still a complex problem in heterogeneous formations (Bilgesu et al., 1993).

### 3.3 Fluids Saturation

Another important reservoir parameter is fluid saturation, which is the fraction of pore space occupied by a certain fluid. Dullien, (1979) expressed the fluid saturation ( $S_i$ ) as follows:

$$S_i = \frac{V_{phase_i}}{V_{pore}} \quad (3.4)$$

Where  $V_{phase_i}$  = Volume of fluid

$V_{pore}$  = Volume constituting the total porosity.

Several authors, including Glover, (2011), state that reservoir rock often contain two (oil and water), or even three (oil, water and gas) fluids phases.

Water saturation can be computed by a number of independent methods, among these are: routine-core analysis, special-core-analysis, capillary pressure data and resistivity measurement that in certain situations is used in combination with special core analysis. The integration of more than one method will result in the most accurate water saturation ( $S_w$ ) overall.

Resistivity measurements have been the most traditional method to determine the hydrocarbon saturation in a reservoir. This method is understood as an indirect method grounded on the differences in conductivity of the water and hydrocarbons. Dissolved salts are present in water formations that enable ionic conductivity whereas hydrocarbons do not conduct (Theodoor, 2000). Moreover, most of the minerals constituting the rock matrix have a very high resistance that allows building the relationship between electric conductivity and saturation (Thomas, 1992).

In the water-saturation calculation using resistivity logs, the connate-brine salinity and its resistivity ( $R_w$ ), can vary within the hydrocarbon column, but the extent of this variation is often not measured. In most conventional water saturation ( $S_w$ ) calculations using well logs, they are both assumed to be constant, and these assumptions can lead to significant errors in the calculated  $S_w$  values. The water saturation ( $S_w$ ) calculated from the resistivity logs and the Archie parameters can be partially checked in aquifer intervals where water saturation ( $S_w$ ) is known to be 100% (Thomas, 1992).

### Archie' equation

Hydrocarbon bearing reservoir conductivity can be measured with resistivity logging tools (Thomas,1992). An interpretation of these measurements has to be done in order to estimate the water saturation which is one of the required parameters to estimate the total amount of hydrocarbons in place. Techlog software there are a lot of saturation computed methods using resistivity, where each of the computation methods are variations of Archie model (Archie, 1950). Arche equation is expressed as follows:

$$R_t = \frac{a \cdot R_w}{\phi^m \cdot S_w^n} \quad (3.5)$$

Where,  $R_t$  = formation resistivity

$R_w$  = water resistivity

$n$  = saturation exponent

$a$  = factor (approximately 1)

$m$  = cementation exponent

$\phi$  = porosity

Water resistivity ( $R_w$ ) is determined in water zone ( $S_w = 1$ ) where  $R_t$  and porosity is read from the logs.

### 3.3 Hydrocarbon volume calculation

Reservoir rocks should have porosity and permeability that allows them to contain a significant amount of extractable hydrocarbons.

The calculation of hydrocarbon volume requires the knowledge of the volume of the formations containing hydrocarbons, the porosity of each formation, hydrocarbon saturation of each formation, the thickness of reservoir rock in the zone ( $h$ ) that can be generated from the petrophysical interpretation defining the zone and the area ( $A$ ) that can be taken from the seismic data.

The product of area of the reservoir ( $A$ ) and the reservoir thickness ( $h$ ) gives the bulk volume of the reservoir ( $V_{bulk}$ ) as seen in the following equation:

$$V_{bulk} = A * h \quad (3.6)$$

Apart of bulk volume of the reservoir, formation factor, both for gas and oil are other important parameters to be considered in hydrocarbon volume calculation. The formation volume factor is

the ratio of the volume of standard mass of gas or oil at reservoir at stock tank condition (Glover, 2011). Therefore, we are in condition to calculate the amount of gas originally in place at a certain pressure and temperature present in the stock tank (Glover, 2011).

$$STGOIP = \frac{43560 * Ah\phi * (1 - S_w)}{B_{gi}} \quad (3.7)$$

Here,

STGOIP = Stock tank gas Initial in place

$A$  = Area of reservoir (Acre)

$h$  = Height or thickness of pay zone (ft)

$S_{gi}$  = Initial gas saturated in the solution (Reservoir bbls/STB)

$S_w$  = Water saturation (%)

$B_{gi}$  = Formation volume factor for gas at initial conditions

$\phi$  = Porosity from the log (%)

All the calculations above should consider the conversions listed in the Table 4.

Table 4 - Standard units used in oil industry

Unit	Equivalent in foot- units	SI Equivalent
1 acre	43560 sq.ft	4047 m
1 barrel (bbl)	5.6154 cu.ft	159 litres
1 acre foot	43560 cu.ft	1233522 litres = 7758 bbl

### 3.4 Uncertainty Estimation

Permeability can be identified in the integrated reservoir description process with a large number of uncertainties because of the input used to determine some of these properties. These uncertainties can be generated from the geological environment, data acquisition and laboratory measurements (Riegert et al., 2007).

According to Ballin (1993), uncertainty is defined as a lack of assurance about the truth of a statement or about the exact magnitude of an unknown measurement or number. The degree of

uncertainty may vary from one variable to another (from exploration phase until the end of life of the reservoir).

The analysis of the uncertainty has been an important tool to use in the study of petroleum reservoirs from its phase of exploration going beyond the production, by offering the possibility to quantify the uncertainties related to reservoir evaluation in all then aspects. Therefore due the number of variable and parameters to be considered the process of this analysis is classified as a complex (William et al., 2011).

The requirements for the petrophysical uncertainty estimation have not been a recent development. Many of the papers describe that Monte-Carlo simulation can be applied for this purposes (Adams, 2005).

### 3.4.1 Monte Carlo simulation

Monte-Carlo simulations enable to model phenomena with significant uncertainty in input and also analyze systems with a large number of coupled degrees of freedom: Fluids, disordered materials, and strongly coupled solids. Using Monte-Carlo simulation the uncertainty in the outputs is determined by randomly selecting input values from their uncertainty distribution applying the sensitive case analyses Liu and Oliver (2003)

Monte Carlo can be used to model probabilistic (or stochastic) systems and set up the odds for a variety of outcomes. Therefore, all the output value is examined statistically to determine the uncertainty in the output values. It works with a class of computational algorithms that rely on repeated random sampling to compute their results (Adams, 2005)

Permeability uncertainty is one of the uncertainty groups when talking about reservoir property uncertainties that played a critical influence in the development of a field.

#### **Tornado Plot**

Tornado plot, also called tornado chart, is a bar chart that compares the relative weight of the variable in a process, a workflow or a computation. It is a bar chart where input data is listed vertically and ordered so that the largest bar appears at the top of the chart, the second largest appears second from the top and the lower bar has a lesser impact (Figure 7). The uncertainty in the parameter or variable is associated to the width of the bar in the plot. This plot is intrinsically related with single factor sensitivity analysis that is defined as meaning the flexing of one or at most two variables to see how these changes affect key outputs, allowing one to test the

sensitivity associated with one uncertainty variable. Once doing the interpretation of the chart, a variable is considered sensitive while others are considered stable (Schlumberger Publication, 2014)

Monte Carlo simulations will be used to characterize the petrophysical uncertainty on permeability. Tornado plots will be used for better understanding of the variable that will influence the permeability output.

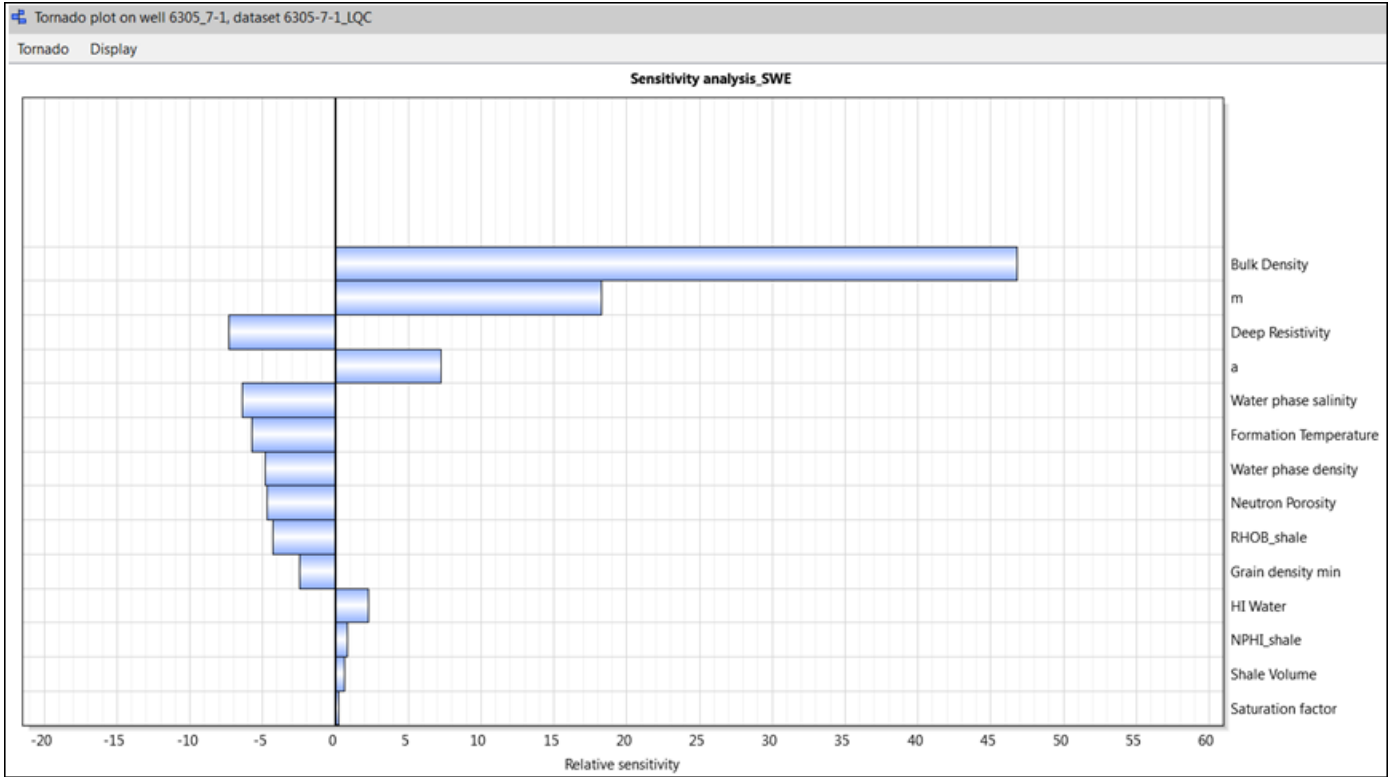


Figure 7: Tornado Plot illustration (Techlog 2013.4)

## **CHAPTER 4- METHODOLOGY**

The Techlog software (well bore platform) was used to integrate all the available wellbore data in order to interpret and compute the input of the different petrophysical properties to deliver a more realistic and accurate formation evaluation.

### **4.1 Provided data**

The entire work was based on a set of existing data provided by the Norwegian University of Science and Technology and Schlumberger provided the software support. The following data were given:

Five wells with the following log data:

Gamma ray (GR)

Density (DEN)

Neutron (NEU)

Deep Resistivity (RDEP)

Micro Resistivity (RMIC)

Acoustic (AC)

Bit size (BS)

### **4.2 Data loading and quality control**

Whilst importing data into Techlog great care was taken for each well and its respective log. Therefore, before importing any type of data it was important to define the same concepts related to importation step:

- Project browser: Shows all the data and Techlog objects loaded in the project
- Import buffer window: The window used to data importation before go to the project browser.
- Well: A group of dataset sharing the same well name.

- Dataset: A group of variable sharing the same reference
- Variable: A group of values (text, value, array, image) where each value represents a reference value of the dataset. They are a series of data (alphanumeric, scalar curves, or vector arrays) arranged according to a chosen index or reference, determined by the dataset that contains the variable.

The data was loaded using a powerful drag-and-drop interface into the Techlog platform. It was taken as an eas way to load the data in Techlog. Afterwords, a logview was created to visualize the curves, validate and correct data for environmental and signal-noise effects, where variable shifting step was done to correct the track.

In general, there are four different ways to import data, which method is used depends on the type of the file:

Drag the files to be imported into Techlog (LAS, DLIS, Techlog XML, CSV files)

Select Project Import from the main Techlog window

Select Home > import

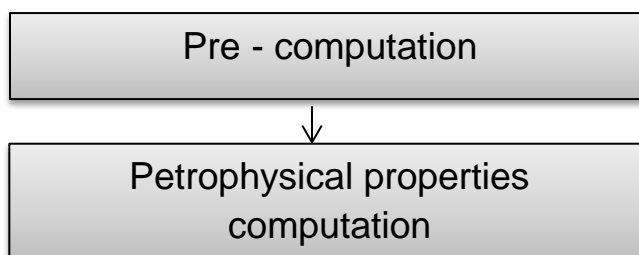
Press Ctrl + Shift + J, I

According to the data type available for this work, the powerfull drag-and-drop interface was used to import buffer window. Before importing the project, a quality check (QC) was done for each data as well.

Prior to performing any petrophysical evaluation in Techlog, a variable should be assigned to a family and unit followed with the workflow. A family is a tag applied to a group of variables that have equivalent characteristics.

#### 4.3 - Workflow implemented to perform the formation evaluation using Techlog

Formation evaluation workflows are composed of several computational methods, where each method is introduced to new tools and concepts. Bearing in mind to the objective and available data, the workflow implemented to perform the formation evaluation is outlined as follow:



#### 4.4 Pre computation workflow

This workflow comprises of bad hole flag and borehole computation. These provide the information about the quality of the bore hole.

##### 4.4.1 Bad hole flag

This module determines the interval where bad hole conditions can corrupt the quality of the measurement especially the density tools. The zones are flagged using the integration of caliper log as a mandatory and bit size as optional input (Table 5). Both caliper and bit size measures the diameter of the borehole (Schlumberger Publications, 2014).

Table 5 - Input Parameters of the bad hole computation

Nome	Unit	Description	Default value
Caliper	In	The measured diameter of a borehole	Mandatory
Bite Size	In	Bit size diameter	Optional

In bad hole method settings (Table 6) in zonation tool bar, it was defined specific interval to which the computations were applied. Thereby, the computation was performed from the top to the bottom of the dataset. Correct values of bit size and cutoff 8.5 and 0.5 inch, respectively for each that dataset were entered into parameter tool bar (Table 7).

Table 6 - Bad hole computation with specific zonation interval

Method settings					
Bad hole flag (Caliper)					
Inputs	Zonation	Parameters			
Zonation name: ZONATION_ALL					
	1	2	3	4	5
Group					
Well	6305_4-1	6305_4-2 S	6305_5-1	6305_7-1	6305_8-1
Dataset	6305-4-1_LQC	6305-4-2S_LQC	6305-5-1_LQC	6305-7-1_LQC	6305-8-1_LQC
Zone	ALL	ALL	ALL	ALL	ALL
Top	2724	2745.1	2670	2823	2857
Bottom	2975.003	2984.521	3052.981	3350	3175.059
Unit	m	m	m	m	m

Table 7 - Bad hole computation parameter set up

Method settings					
Bad hole flag (Caliper)     					
Inputs	Zonation	Parameters			
	1	2	3	4	5
Group					
Well	6305_4-1	6305_4-2 S	6305_5-1	6305_7-1	6305_8-1
Dataset	6305-4-1_LQC	6305-4-2S_LQC	6305-5-1_LQC	6305-7-1_LQC	6305-8-1_LQC
Zone	ALL	ALL	ALL	ALL	ALL
Top	2724	2745.1	2670	2823	2857
Bottom	2975.003	2984.521	3052.981	3350	3175.059
Bit Size	8.5	8.5	8.5	8.5	8.5
Bit Size unit	in	in	in	in	in
Cutoff	0.5	0.5	0.5	0.5	0.5
Cutoff unit	in	in	in	in	in

Bad hole computation uses algorithm tests, if the difference between the caliper and the bit size diameter is greater than the user-defined cut off. The possible values for bad hole flag are 0 and 1

After setting all the information and running the computation the new curve will appear named BH\_FL\_BS as a discrete log in each dataset as output variable of this computation.

#### 4.4.2 Borehole computation

In this section, a number of computations were done including temperature, pressure and salinity. An option is provided to convert parameters to variables and also to adjust all parameters according to the input data.

The borehole computation is accurate if it is used with a true vertical depth (TVD) reference. It is recommended to run a TVD computation before any borehole computation if the reference is in measured depth (MD), whilst doing the borehole computation, the borehole temperature, true vertical depth (TVD) are a mandatory input to be set up, while borehole pressure, mud resistivity are set as optional inputs (Table 8)

Table 8 - Borehole computation input

Nome	Unit	Description	Default Value
<b>True vertical depth (TVD)</b>	m	This is used for the computation of temperature and pressure (Ideally TVD below the mud-line)	Mandatory
<b>Borehole temperature</b>	degC	This circumvents temperature computation	Optional
<b>Borehole Pressure</b>	Kpa	This circumvents pressure computation if a borehole pressure is available	Optional
<b>Mud resistivity</b>	Ohm-m	This circumvents mud resistivity	Optional

#### 4.5 Petrophysical properties computation

This workflow consists of lithology determination, shale volume, total porosity, saturation, effective porosity, permeability and summaries computation.

#### 4.5.1 Lithology Determination

One of the main applications of the density log is to determinate the porosity. In addition, when used in combination with neutron porosity, it is used to determine the lithology (sand, limestone, anhydrite and dolomite).

There are two main ways to determine the lithology using density-neutron cross plot.

- ❖ Multi-well cross plot, allows comparison of data from more than one well.
- ❖ Single-well cross-plot, allows handling multiple scales and multiple variables.

In this work the single well cross plot Neutron Porosity vs Bulk Density (TNPH) was chosen to better understand the contribution of each well and proportion of each lithology type drilled in each well.

The Neutron-density cross-plot presents two axis, x and y. On the x-axis of the cross-plot is neutron and bulk density is on the y-axis. The intersection between two values gives the porosity and lithology (Figure 9)

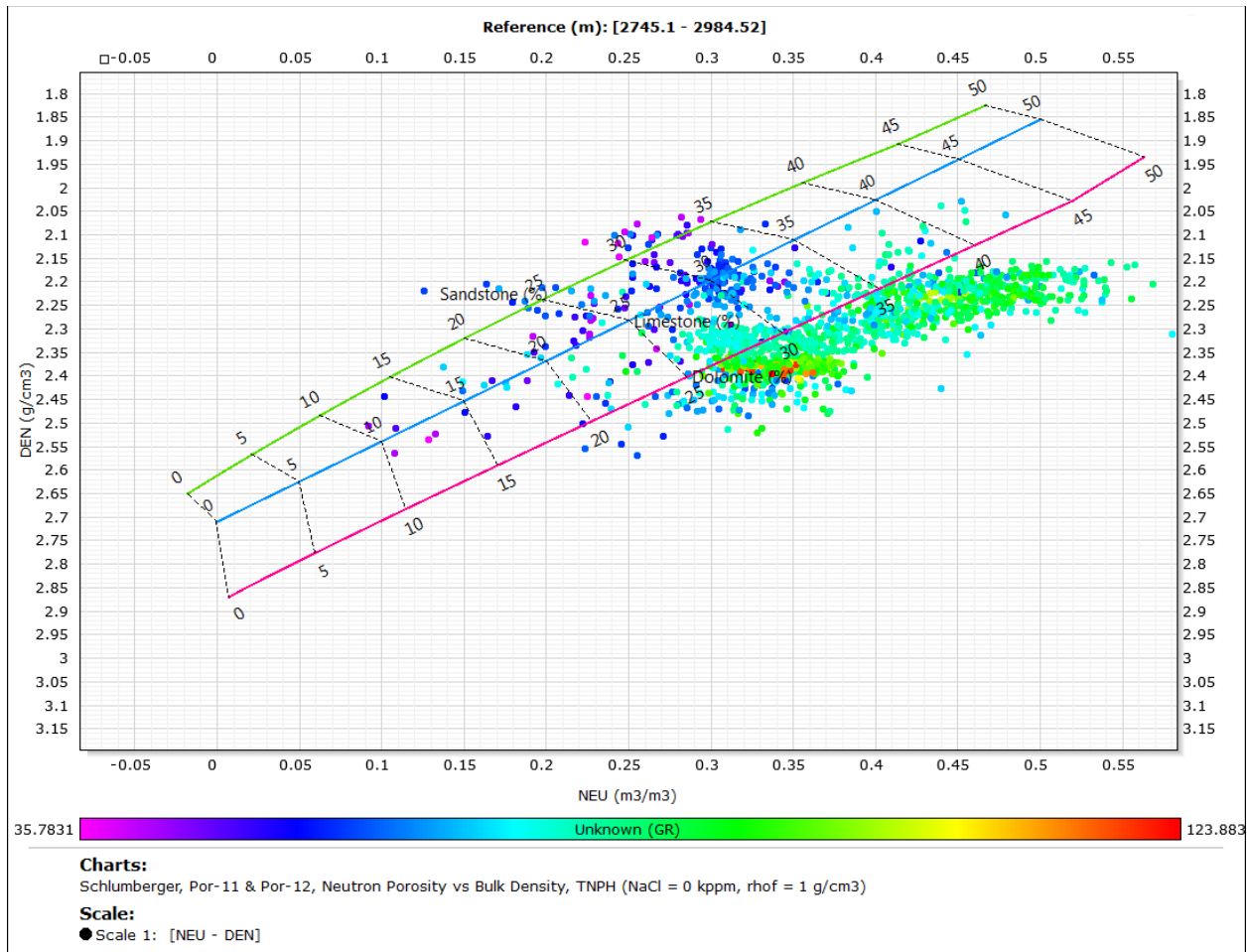


Figure 8: Neutron-density cross-plot (Techlog 2013.4)

In the summaries computation module the average of the shale volume, porosity and water saturation was computed in order to define the reservoir interval pay zone.

#### 4.5.2 Shale Volume Computation

Shale volume computation determines the amount of shale in percentage using Gamma ray log. This computation is important because it gives an idea of how much shale presence can affect the effective porosity, fill the porous space and decrease space for hydrocarbons. However, to calculate the V<sub>sh</sub> in the reservoir zone of all of the well was applied 40% and 100% as a GR<sub>matrix</sub> and GR<sub>shale</sub> respectively.

Shale volume can be computed using combined and individual methods. In this project it was used the combined method.

### Combined method

This method covers most of the usual shale volume computation into one method using gamma ray index ( $GR_{index}$ ) coming from different approximation method, like linear, larionove, clavier, steiber and gamma ray curve ( see equation 4.1). Linear approximation method was the preferred method for shale volume.

$$GR_{index} = \frac{GR - GR_{matrix}}{GR_{shale} - GR_{matrix}} \quad (4.1)$$

Where  $GR_{matrix}$  = gamma ray log reading in 100% matrix rock

$GR_{shale}$  = gamma ray log reading in 100% shale

$GR$  = gamma ray at specific depth.

One of the advantages to use the combined method is the possibility of running different methods in one and gives just one  $V_{sh}$  result, whereas using separate methods to combine gamma ray, density and thermal neutron or electromagnetic propagation 4 or 5 methods must be run from the same workflow.

At the end of the shale volume computation a final shale volume (VSH Final) is automatically computed. The final shale volume is a combination of different volume of shale computed from different proposed mean: Arithmetic means: Arithimetric mean, Geometric mean, Harmonic mean, Median, minimum, first present, product and sum.

### 4.5.3 Total Porosity and Saturation from Neutron- Density

The total porosity and saturation from neutron-density method computes total porosity (PHIT) in virgin and invaded zone water saturation (SWT and SXOT). From these parameters: neutron, density, true resistivity and, water volume fraction, dry shale volume and bound water volume. Table 9 illustrates the optional and mandatory inputs variable.

Techlog uses Equation 4.2 to calculate total porosity:

$$\phi_T = \frac{\rho_{ma} - \rho_B}{\rho_{ma} - \rho_f} \tag{4.2}$$

Here,  $\rho_{ma}$  is density log reading in 100% matrix rock, default 2.65,  $\rho_f$  is fluid density,  $\rho_B$  is density log reading in zone of interest.

Table 9 - Input variable for total porosity and saturation

Nome	Unit	Description	Default Value
Neutron Porosity	v/v	Neutron porosity log reading (limestone porosity units).	Mandatory
Bulk Density	g/cm3	Bulk Density log reading.	Mandatory
Shale Volume	v/v	Shale Volume (assumed hydrated as this is an effective porosity computation )	Mandatory
True Formation Resistivity	Ohm.m	True Resistivity Log. Required of unflushed zone saturation.	Optional
Flushed Formation Resistivity	Ohm.m	Micro Resistivity Log. Required for flushed zone saturation.	Optional
Formation Water Resistivity	Ohm.m	Water Resistivity of the formation.	Optional
Temperature	degF	Temperature of the formation.	Mandatory
Pressure	Psi	Pressure of the formation.	Mandatory
General Flag	unitless	Flag for special minerals or bad hole. No computation is performed where flag=1.	Optional

The advantage of using this method is to make shale and hydrocarbons corrections only if necessary.

#### 4.5.4 Effective Porosity from Neutron-Density

This method computes effective porosity and lithology based on neutron and density. The calculation of effective porosity and lithology runs in a single process with the lithology in part driving the porosity calculation. Using the mandatory and optional input variables listed on Table 10, this method applies the following steps:

The first estimation of the effective porosity is based on the neutron and density tools.

The lithology computation is based on the effective porosity (PHIE and effective invaded water saturation (SXOE) already computed.

The apparent matrix density is calculated based on the lithology already computed on the step before using the mineral volume fraction and apparent mineral matrix density.

A new effective porosity is calculated from density tool (RHOB) based on the new apparent matrix density (RHOMA).

Generally in Techlog all neutron density methods are ran with the same algorithm and the neutron tool (Schlumberger tool) must be calibrated in limestone unit. Effective porosity can be derived from Equation 4.2 and to decide the lithology line it uses the following statements:

If  $\phi_n \leq \phi_d$ , choose Limestone/Sandstone combination

If  $\phi_n \leq \phi_d$ , choose Limestone/Dolomite combination

If

Porosity density calculation Equation 4.3

$$\phi_d = \frac{\rho_b - \rho_{lim}}{\rho_{mf} - \rho_{lim}} \quad (4.3)$$

Where  $\rho_b$  is bulk density,  $\rho_{lim}$  is limestone grain density, default 2.71 g/cm<sup>3</sup>,  $\rho_{mf}$  is mud filtrate density, default 1 g/cm<sup>3</sup> or bulk density fluid parameter,  $\rho_{sand}$  is sandstone grain density, default 2.65 g/cm<sup>3</sup>.

Table 10 - Input Variable for Effective porosity and saturation computation

Nome	Unit	Description	Default Value
Neutron Porosity	v/v	Neutron porosity log reading (limestone porosity units).	Mandatory
Bulk Density	g/cm3	Bulk Density log reading.	Mandatory
Shale Volume	v/v	Shale Volume (assumed hydrated as this is an effective porosity computation )	Mandatory
True Formation Resistivity	Ohm.m	True Resistivity Log. Required of unflushed zone saturation.	Optional
Flushed Formation Resistivity	Ohm.m	Micro Resistivity Log. Required for flushed zone saturation.	Optional
Formation Water Resistivity	Ohm.m	Water Resistivity of the formation.	Optional
Temperature	degF	Temperature of the formation.	Mandatory
Pressure	Psi	Pressure of the formation.	Mandatory
General Flag	unitless	Flag for special minerals or bad hole. No computation is performed where flag=1.	Optional

#### 4.5.5 Permeability computation

Techlog incorporated several equations to compute permeability based on different petrophysical parameters. Among these, the Coates method was chosen to be more accurate and appropriate for the given data. This method uses the following equation:

Clean zones

$$PERM = kc * PHLe^4 * \left(\frac{1-swirr}{swirr}\right)^2 \tag{4.4}$$

Else

$$PERM = kc * PHLe^4 * \left(\frac{PHLt - PHLe*Swirr}{PHLe*swirr}\right)^2 \tag{4.5}$$

As a mandatory variable input for this method effective porosity and total porosity and irreducible water saturation have to be given as optional inputs (Table 11)

Table 11- Permeability input parameter

Nome	Unit	Description	Default Value
Effective Porosity	v/v	Calculated effective porosity	Mandatory
Total Porosity	v/v	Calculated total porosity	Mandatory
Irreducible	v/v	Calculated irreducible water saturation	Optional

#### 4.5.6 Summaries

Summaries compute the average of computed shale volume, porosity and saturation by applying cutoff and flag criteria of rock (Rock), reservoir (Res) and pay (Pay).

Rock flag is computed from volume shale cutoff. Reservoir flag (RES) is computed from volume of shale and porosity cutoff. Pay flag is computed from volume of shale, porosity and water saturation cutoff (Table 12).

Table 12 - Reservoir flag Cutoff

	Flag Name	Flag shading colour	Shale Volume cutoff	Porosity cutoff	Water Saturation cutoff
1	ROCK	Yellow	yes	no	no
2	RES	Green	yes	yes	no
3	PAY	Red	yes	yes	yes

## CHAPTER 5- ANALYSIS AND RESULTS

### 5.1 Lithology Determination

The lithology of the five given wells was determined using the neutron versus density cross - plots.

Figure 10 shows the cross-plot neutron versus density of the well 6305\_4-1, which displays the lithology present in the entire well. Most cloud point is populated on the shale and sandstone region and minor in limestone region, which possibly indicates the presence of calcareous shale. When plotted only the reservoir section points, it clearly indicates a predominance of clean sandstone (Figure 11).

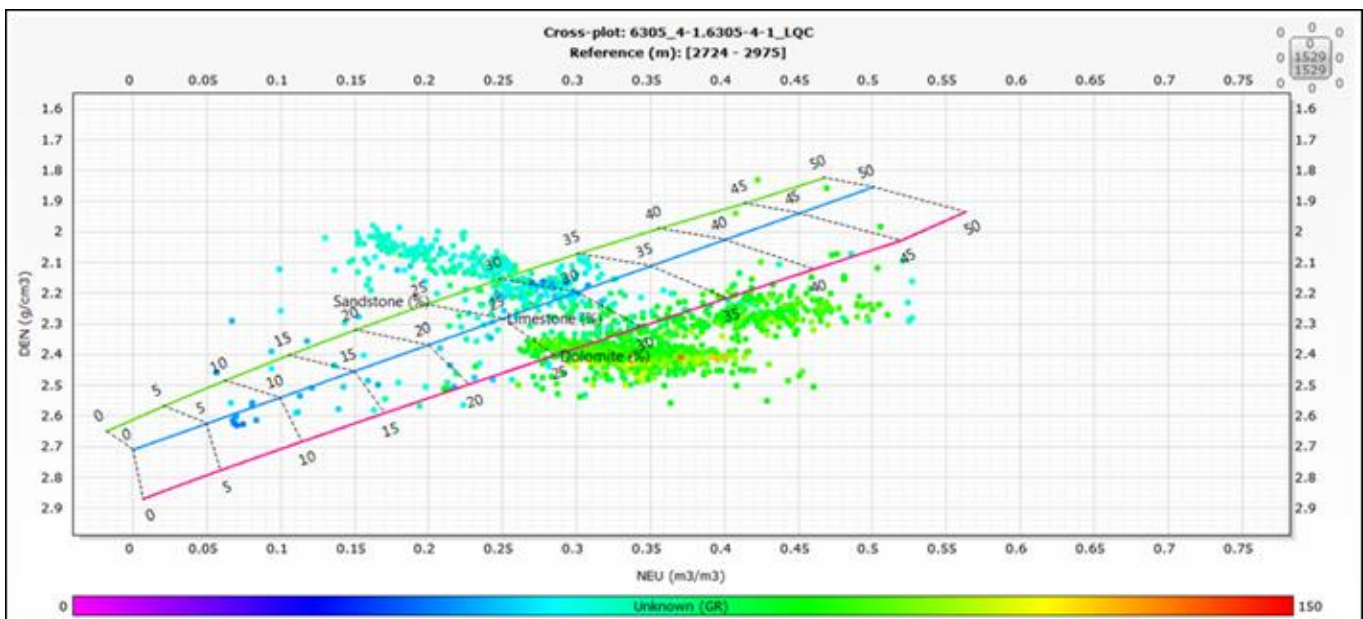


Figure 9: Cross plot Neutron Porosity vs Bulk Density (TNPH) for well 6305\_4-1(Techlog 2013.4)

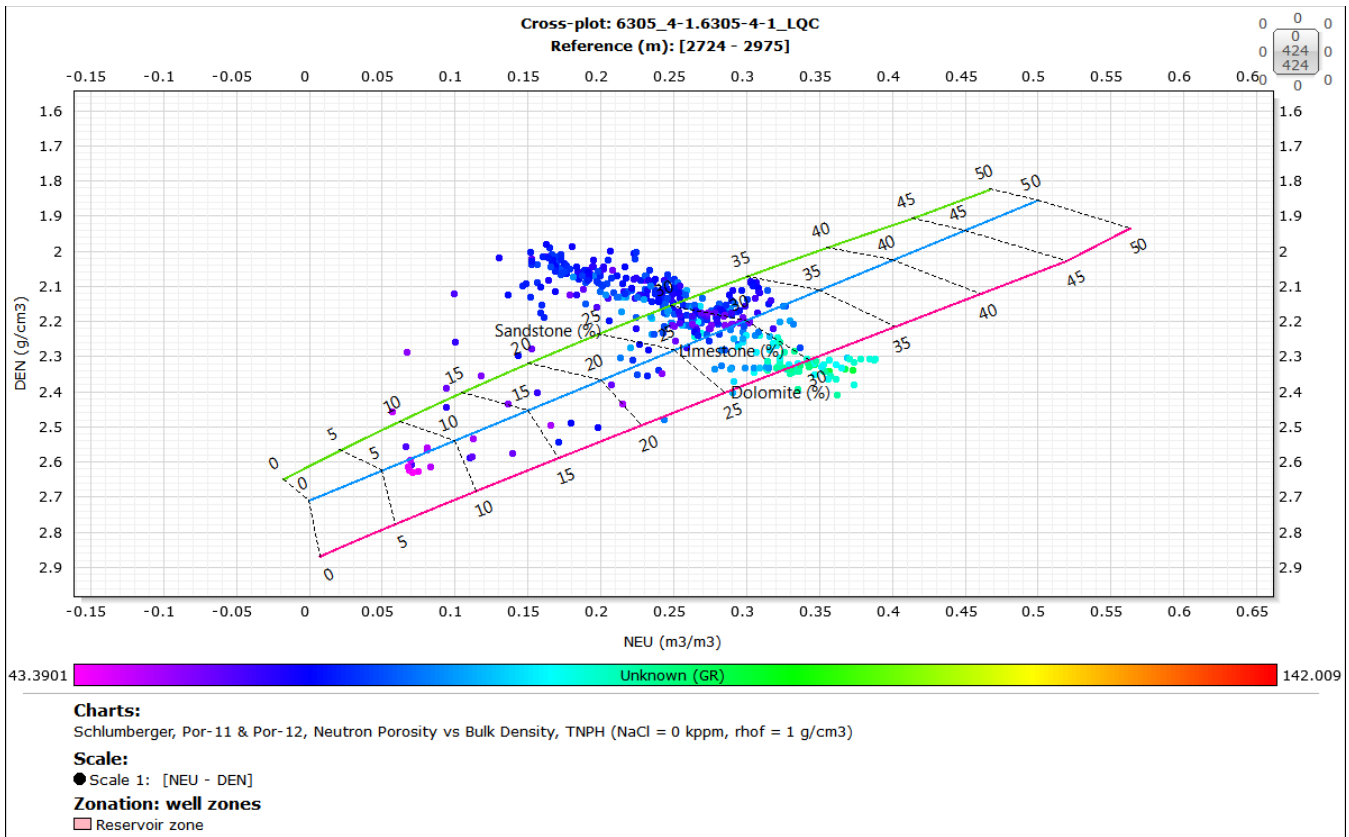


Figure 10: Cross plot Neutron Porosity vs Bulk Density (TNPH) for well 6305\_4-1(Techlog 2013.4)

Figure 12 shows the cross-plot of neutron versus density, for the well 6305\_4-2S which displays the lithology present in the entire well. Most cloud point is populated on the shale regions and minor in sandstone and limestone regions. The points spotted on the limestone region possibly indicate the presence of calcareous shale. When plotted only the points on reservoir section, it clearly indicates a predominance of sandstone mixed with shale (Figure 13).

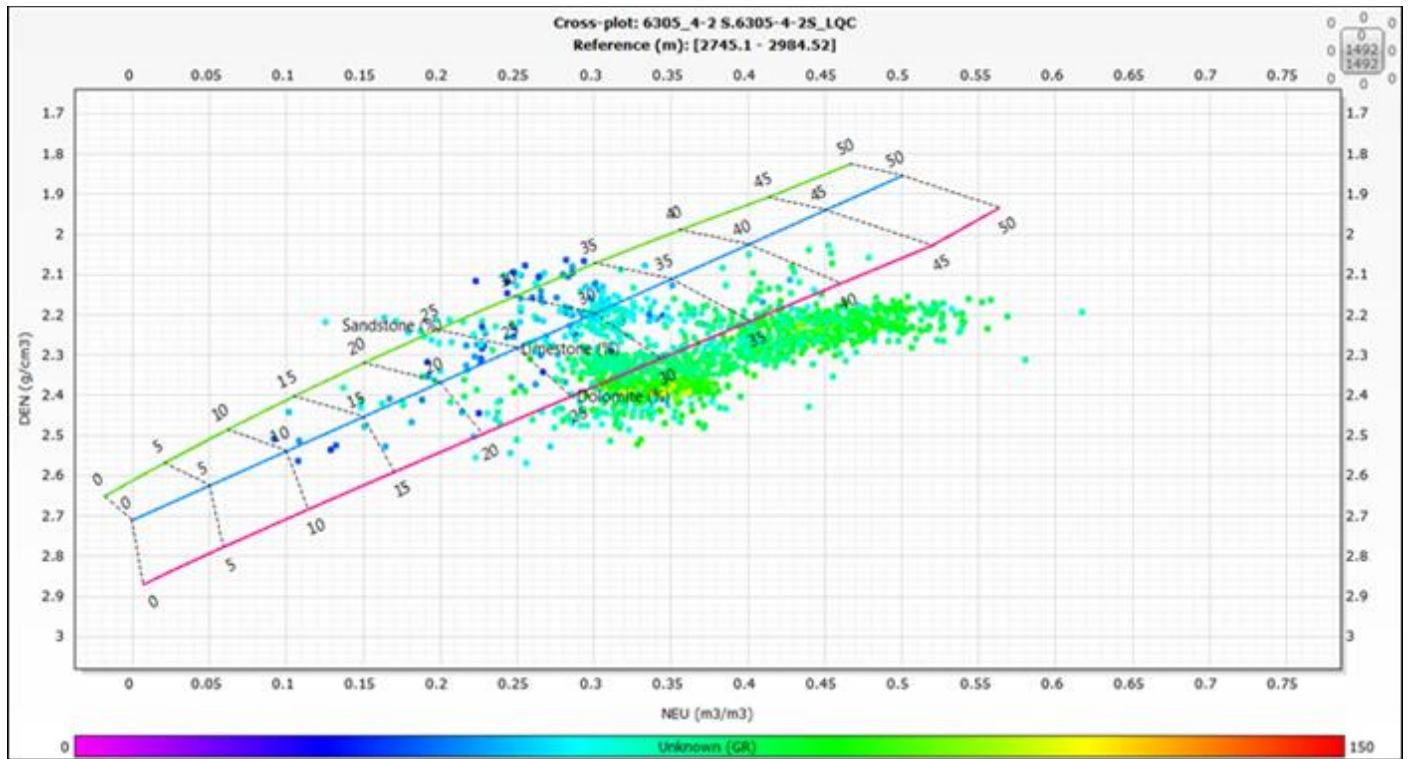


Figure 11: Cross plot Neutron Porosity vs Bulk Density for well 6305\_4-2S (Techlog 2013.4)

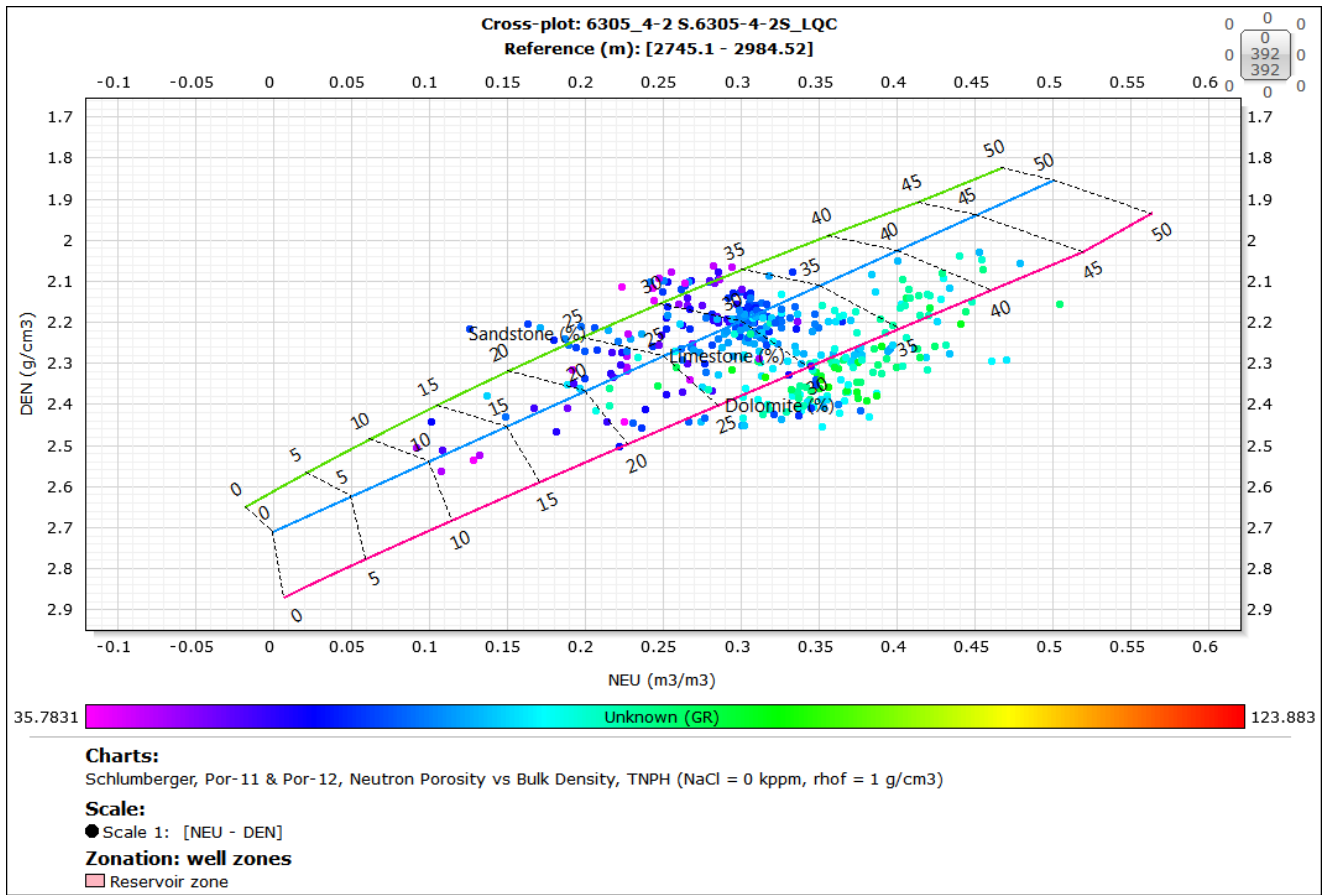


Figure 12: Cross plot Neutron Porosity vs Bulk Density (TNPH) for well 6305\_4-2S (Techlog 2013.4)

Figure 14, shows the cross-plot neutron versus density of the well 6305\_5-1, which displays the lithology present on the entire well. Most cloud point is populated on shale regions and minor in sandstone and some scattered in the limestone region. When plotted only the reservoir section, it clearly indicates a dominant presence of clean sandstone (Figure .15).

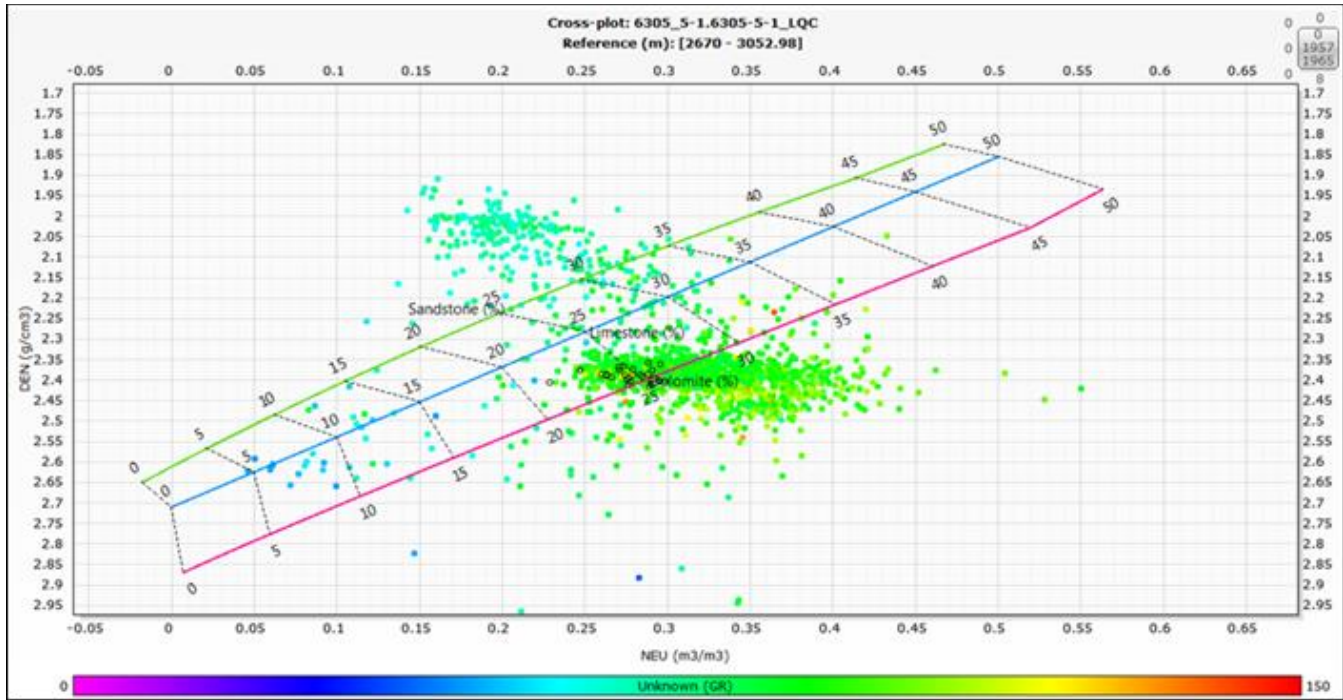


Figure 13: Cross plot Neutron Porosity vs Bulk Density (TNPH) for well 6305\_5-1 (Techlog 2013.4)

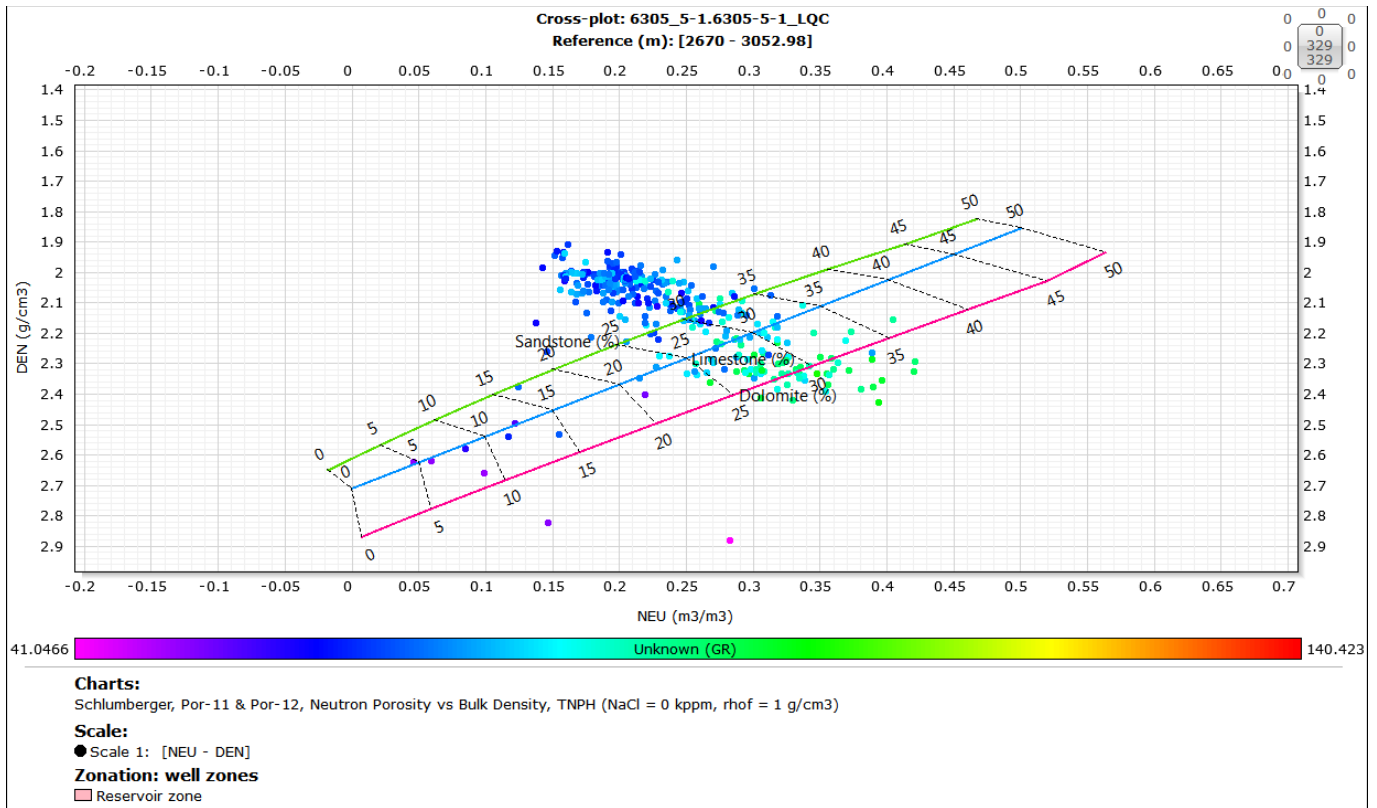


Figure 14: : Cross plot Neutron Porosity vs Bulk Density (TNPH) for well 6305\_5-1 (Techlog 2013.4)

Figure 16, shows the cross-plot neutron versus density of the well 6305\_7-1, which displays the lithology present on the entire well. Most cloud point is populated in the shale region and minor point in the sandstone and some scattered on limestone region. When plotted only the reservoir section points, unlike the other wells, it indicates a presence of sandstone mixed with shale and limestone (Figure 17)

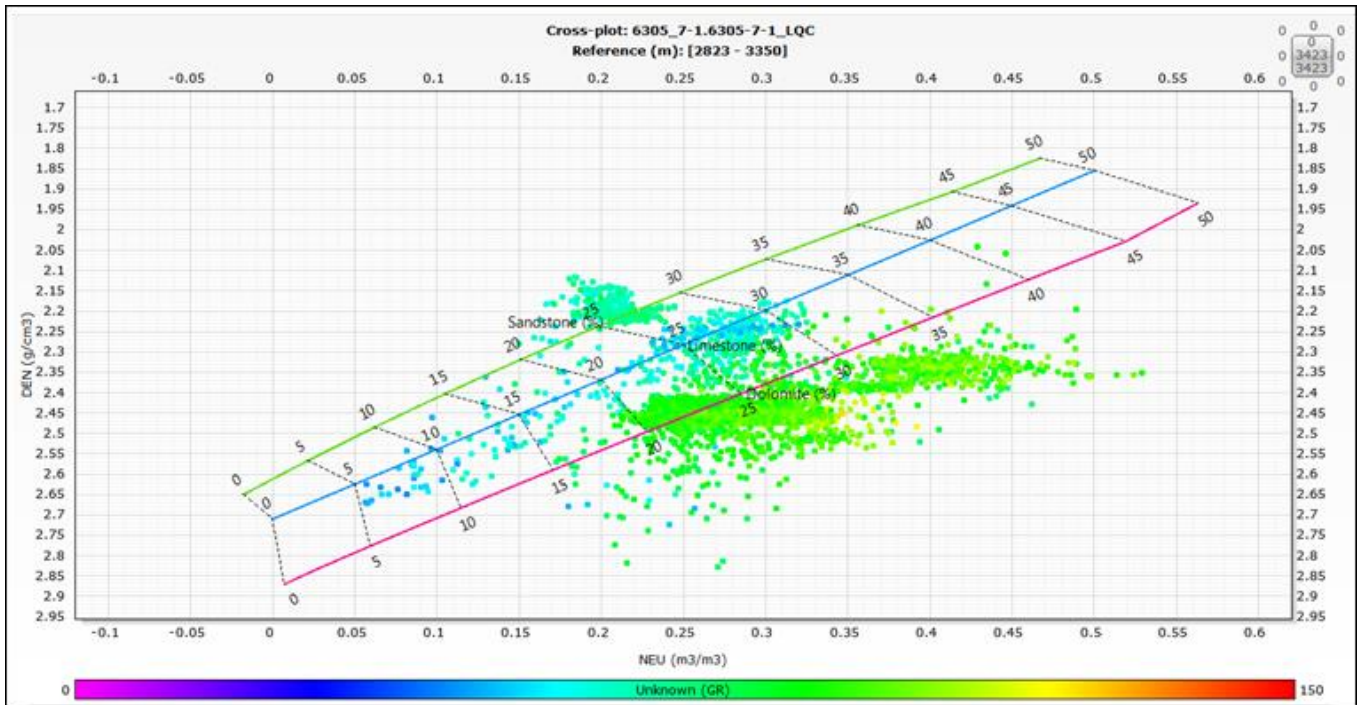


Figure 15: : Cross-plot, Neutron Porosity vs Bulk Density (TNPH) for well 6305\_7-1 (Techlog 2013.4)

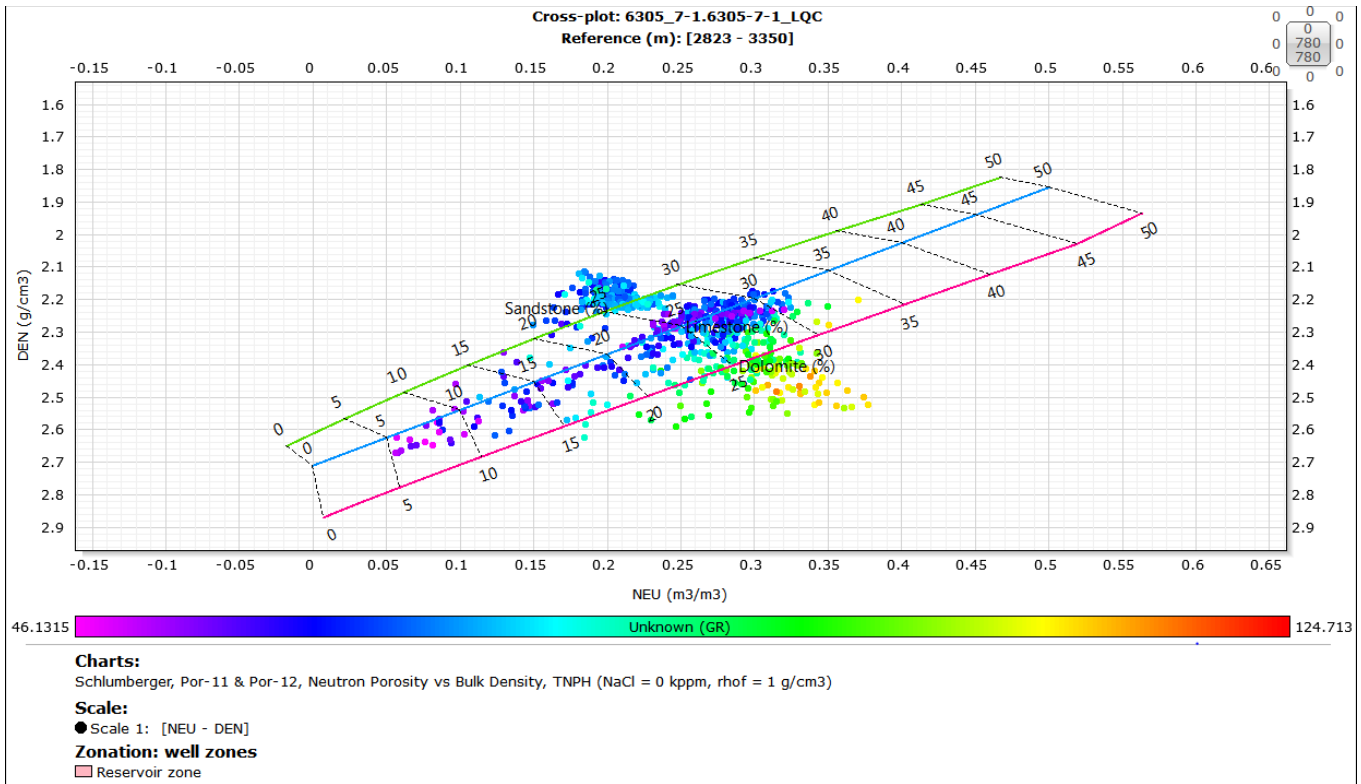


Figure 16: Cross plot Neutron Porosity vs Bulk Density (TNPH) for well 6305\_5-1 (Techlog 2013.4)

Figure 18 shows the cross-plot neutron versus density of the well 6305\_8-1. Most cloud point is populated on the shale region and minor in the limestone and few in sandstone and some scattered in limestone region. When plotted only the reservoir section points, it indicates a the presence of sandstone mixed with shale and limestone (Figure.19).

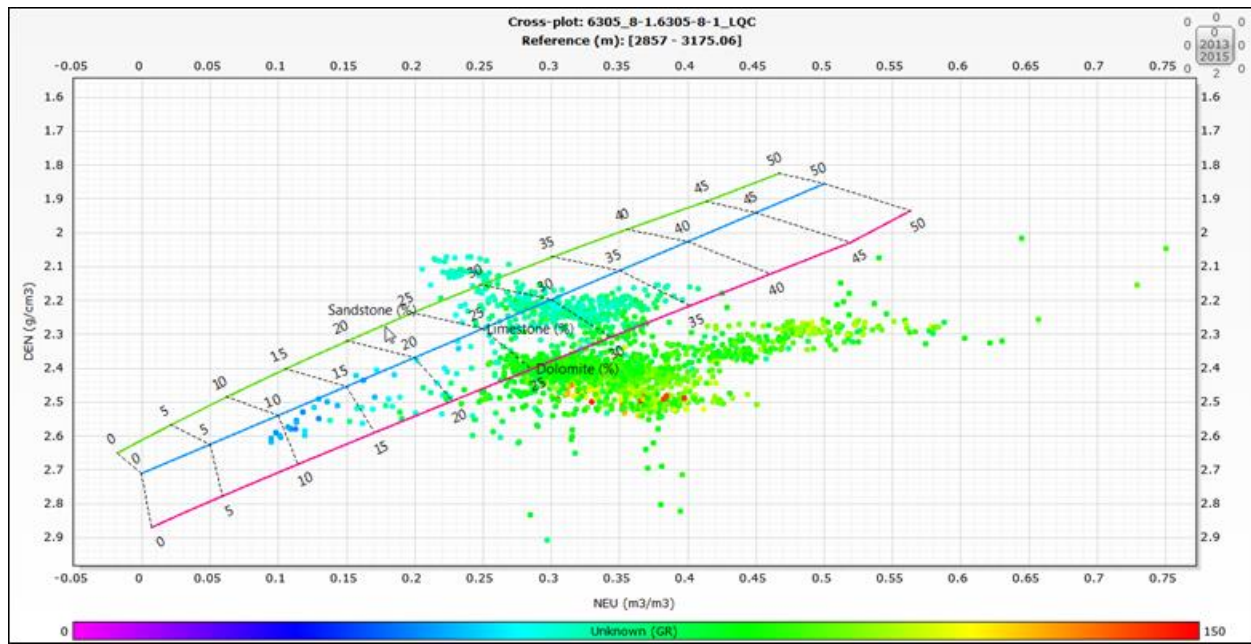


Figure 17: : Cross-plot, Neutron Porosity vs Bulk Density (TNPH) for well 6305\_8-1 (Techlog 2013.4)

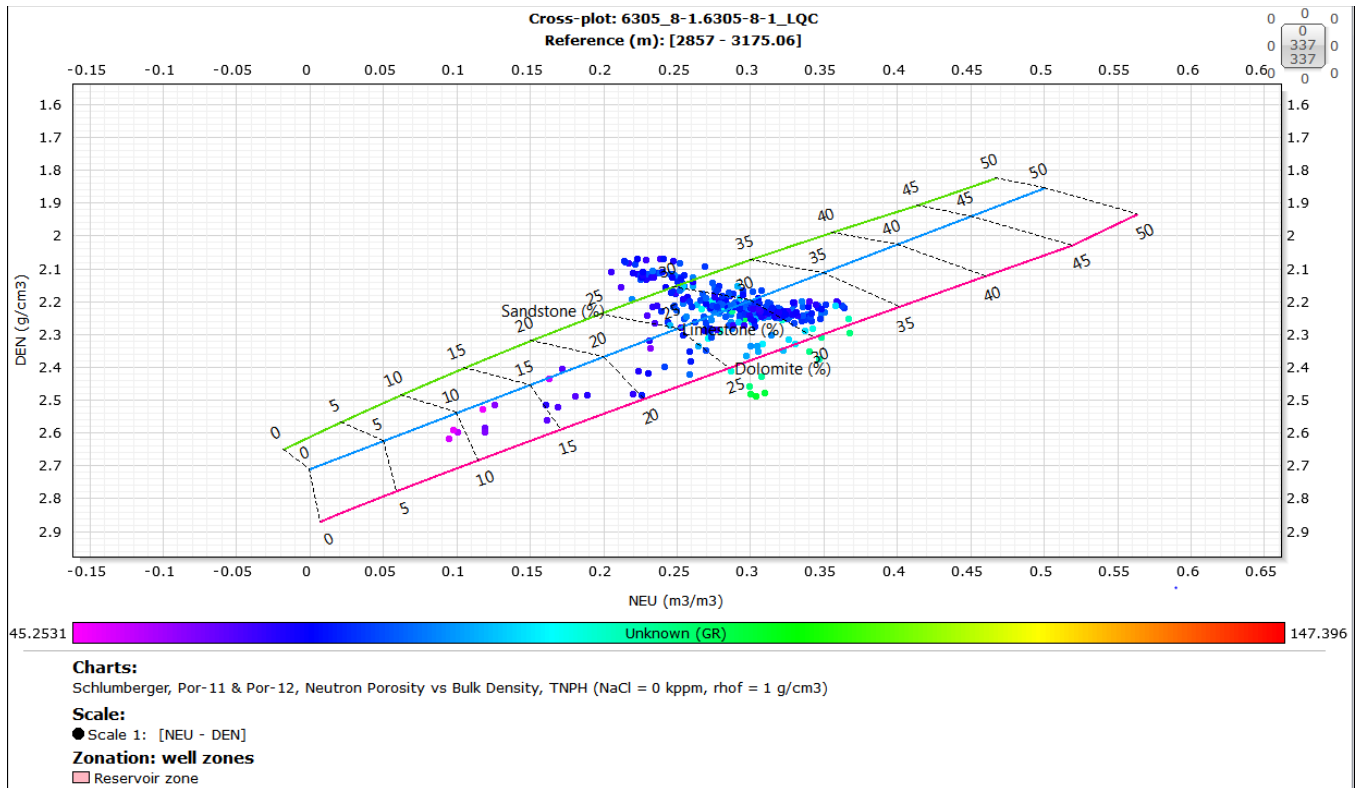


Figure 18: Cross-plot, Neutron Porosity vs Bulk Density (TNPH) for well 6305\_8-1 (Techlog 2013.4)

## 5.2 Zonation

The zonation determination allowed a division of the logs into different zones. The gamma-ray log was used as a shale indicator, density and neutron log as porosity, gas and shale indicators and resistivity log as a fluid indicator. The gamma-ray log was used to define the formation thickness of each well. The five wells presented in this work, are described below, where, are divided into three zones: top zone, reservoir zone and bottom shale.

**Top shale:** This zone was classified lithologically as shale zone because of the very high gamma-ray values encountered in the top of well section.

**Reservoir zone:** This zone was classified lithologically as shaly sand because of the evidence of shale intercalated with sand in some reservoirs. This zone was also characterized by its high resistivity and low gamma ray values, implying the presence of less clay mineral. The reservoir zone was subdivided in two zones: gas zone (R.G.Z) and reservoir bottom zone (R.B.Z). The first zone is also called gas-bearing reservoir zone. In this zone the density-neutron cross-over shows

mirror effect that provides conclusive evidence of gas indication, while, the second zone is filled dominantly with water, though, some gas content is present as evidenced by very low resistivity in this zone.

Bottom shale: This zone is similar to the top zone, the difference is that it is the below the reservoir or in the bottom part of the well section.

### **Well 6305\_4-1**

The thickness of the top shale zone is about 45m. From 2769 m gamma-ray value started gradually decreasing, indicating a transition from shale to reservoir zone. The entire reservoir interval is about 65 m thick. The reservoir gas bearing zone is about 45 m thick where it was marked the gas water contact (GWC) at 2814.22m. The interval thickness of the bottom shale zone is from 2834m to 2974m which is characterized by sharp increase of gamma-ray values (Figure 20).

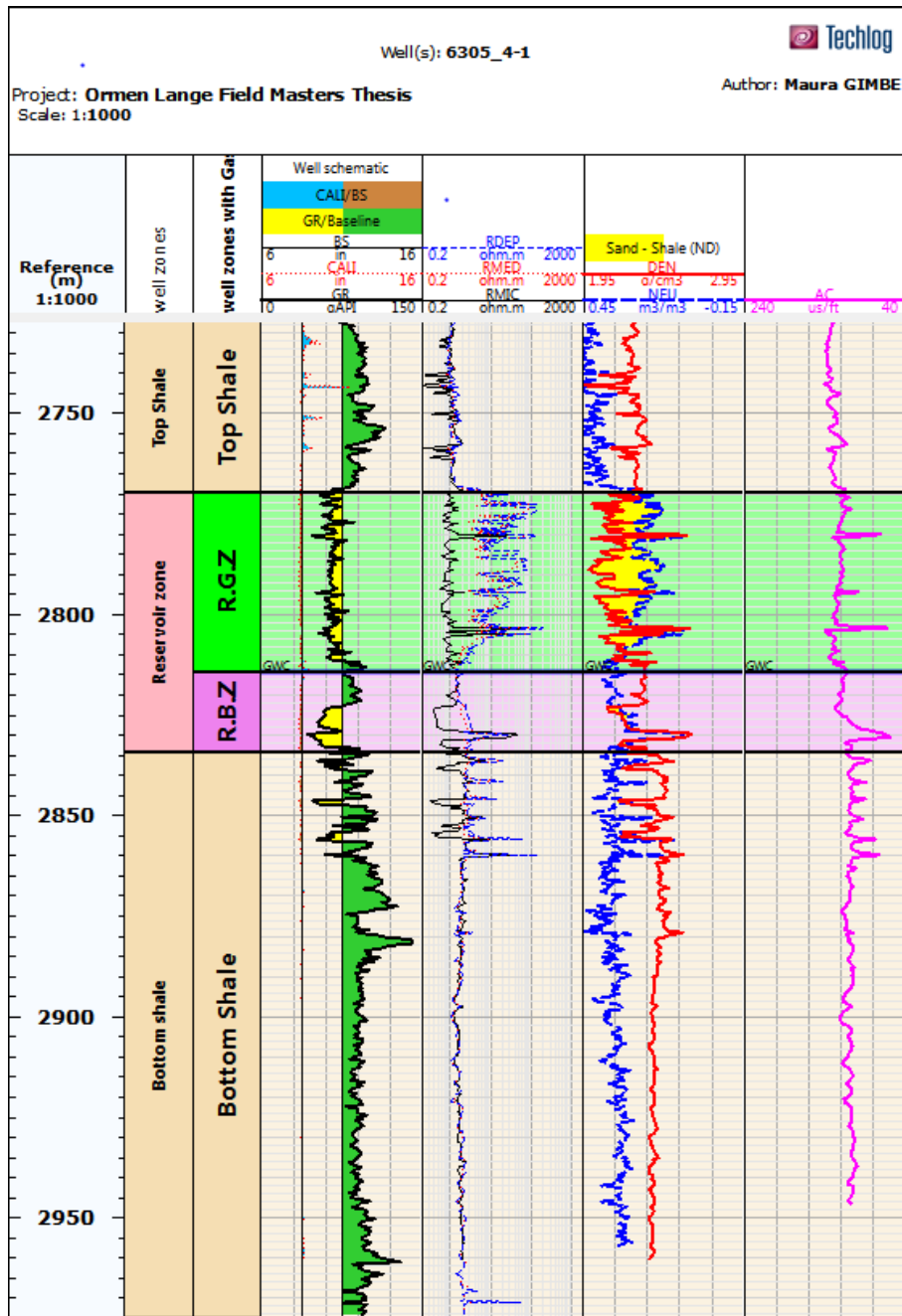


Figure 19: Well zone description for well 6305\_4-1

### Well 6305\_4-2 S

The thickness of the top shale zone is about 45m. From 2834 m the gamma-ray values are gradually decreasing, indicating a transition from shale to reservoir zone. The entire reservoir

interval is about 59 m thick. The reservoir gas bearing zone is about 27 m thick where it was marked the gas water contact (GWC) at 2862m. The interval thickness of the bottom shale zone is from 2894m to 2984m which is characterized by sharp increase of gamma-ray values (Figure 21).

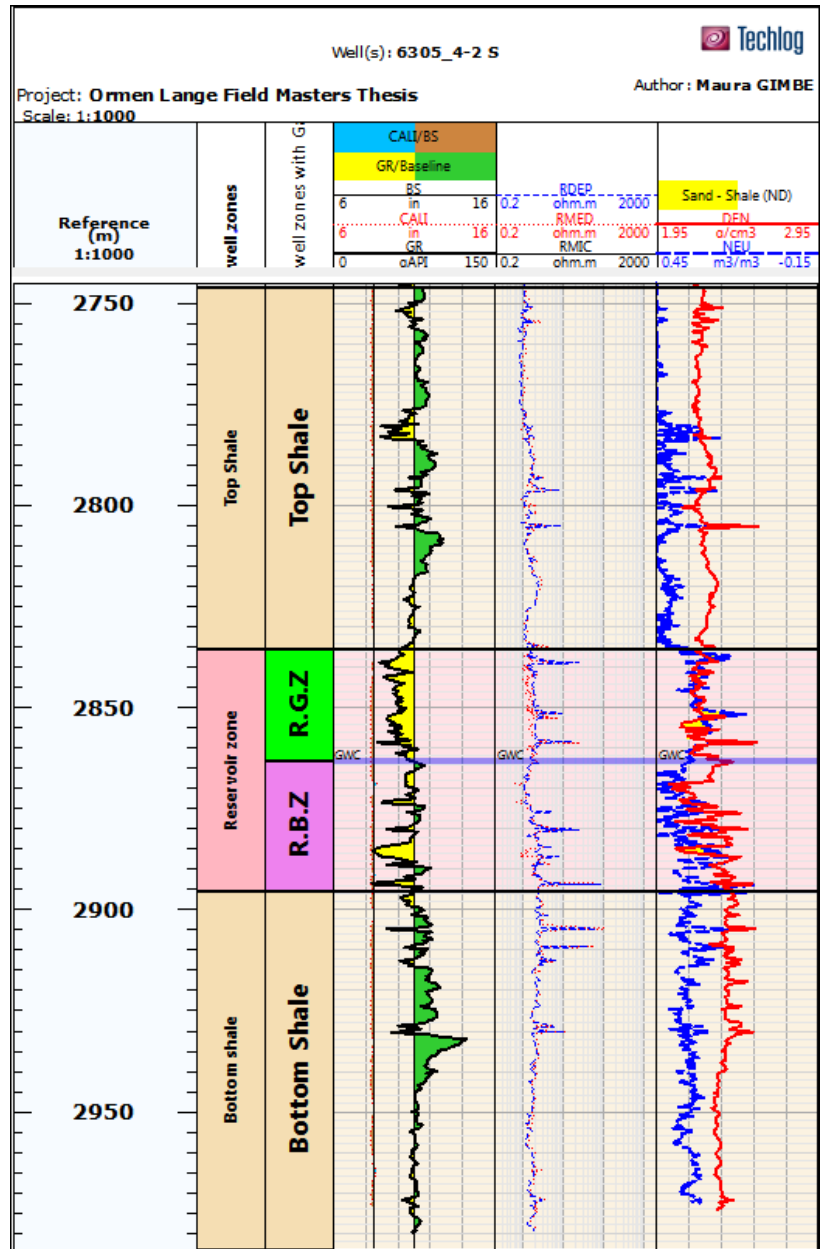


Figure 20: Well zone description for well 6305\_4-2S

## Well 6305\_5-1

The thickness of the top shale zone is about 47m. From 2717 m the gamma-ray values are gradually decreasing, indicating a transition from shale to reservoir zone. The entire reservoir interval is about 62 m thick. The reservoir gas bearing zone is about 49 m thick where it was marked the gas water contact (GWC) at 2766m. The interval thickness of the bottom shale zone is from 2779m to 2905m which is characterized by sharp increase of gamma-ray values (Figure 22).

For unknown reasons, the neutron curve was not seen from the top of shale zone to 2730 m. This affected the effective porosity, permeability, gas saturation, water saturation computation and so on (2670 m to 2733 m ).

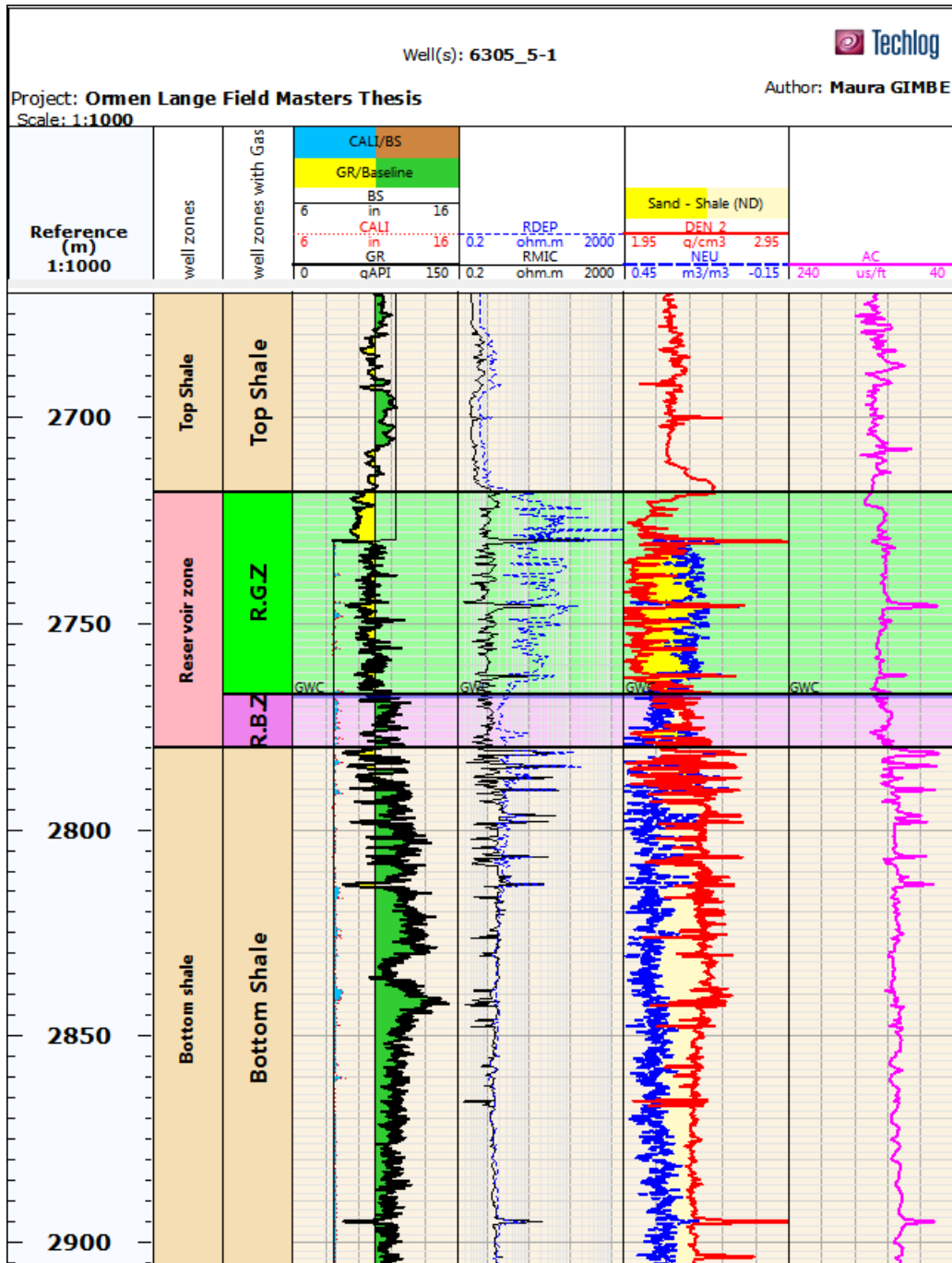


Figure 21: Well zone description for well 6305\_5-1

### Well 6305\_7-1

The thickness of the top shale zone is about 86m. From 2908m gamma-ray values are gradually decreasing, indicating a transition from shale to reservoir zone. The entire reservoir interval is about 119 m thick. The reservoir gas bearing zone is about 41 m thick where it was marked the gas water contact (GWC) at 2949m. The interval thickness of the bottom shale zone is from 3028m to 3350m, which is characterized by sharp increase of gamma-ray value (Figure 23).

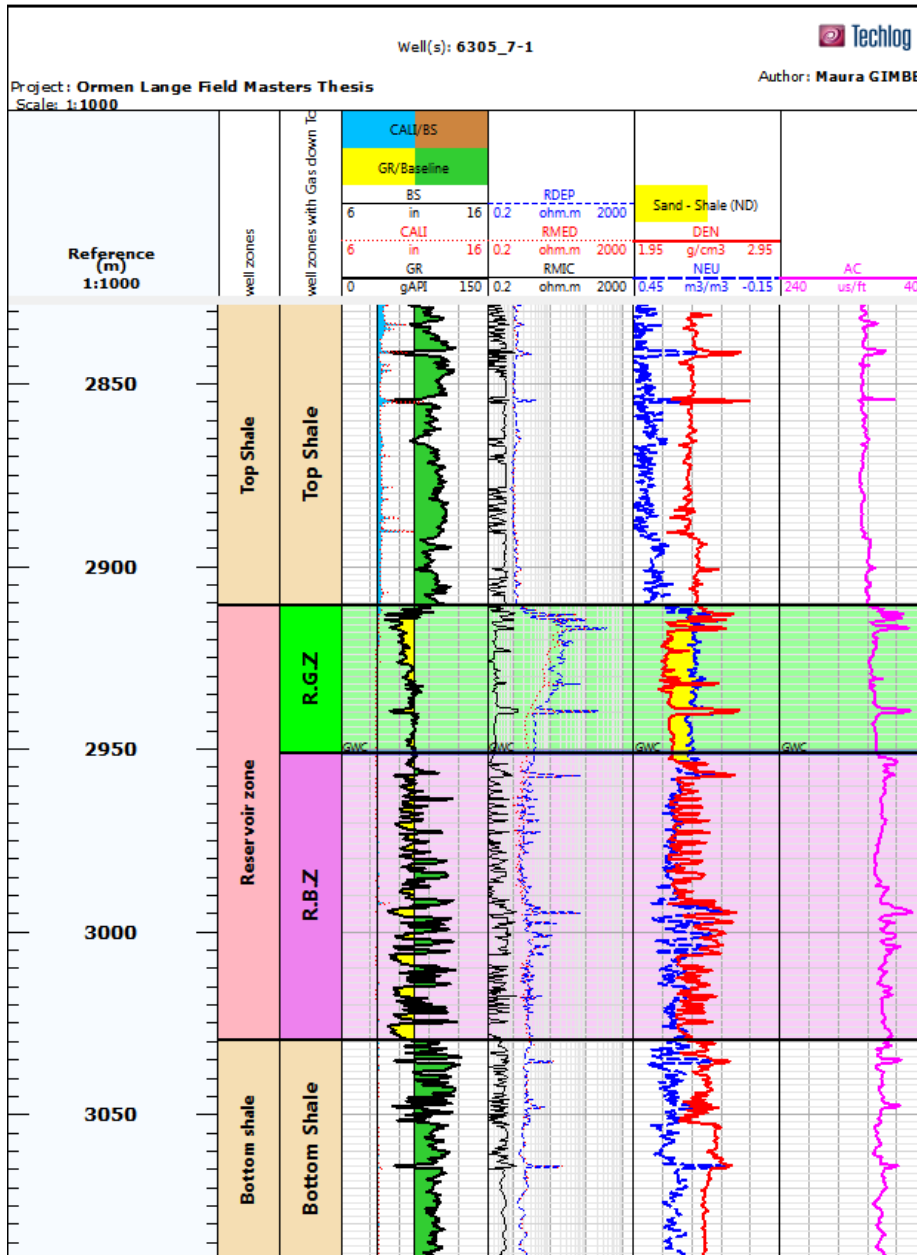


Figure 22: Well zone description for well 6305\_7-1

### Well 6305\_8- 1

The thickness of the top shale zone is about 39m. From 2897 m the gamma-ray values gradually decreasing, indicating a transition from shale to reservoir zone. The entire reservoir interval is about 53 m thick. The reservoir gas bearing zone is about 26 m thick where it was marked the gas water contact (GWC) at 2923m. The interval thickness of the bottom shale zone is from 2949m to 3089m, which is characterized by sharp increase of gamma-ray values (Figure 24).

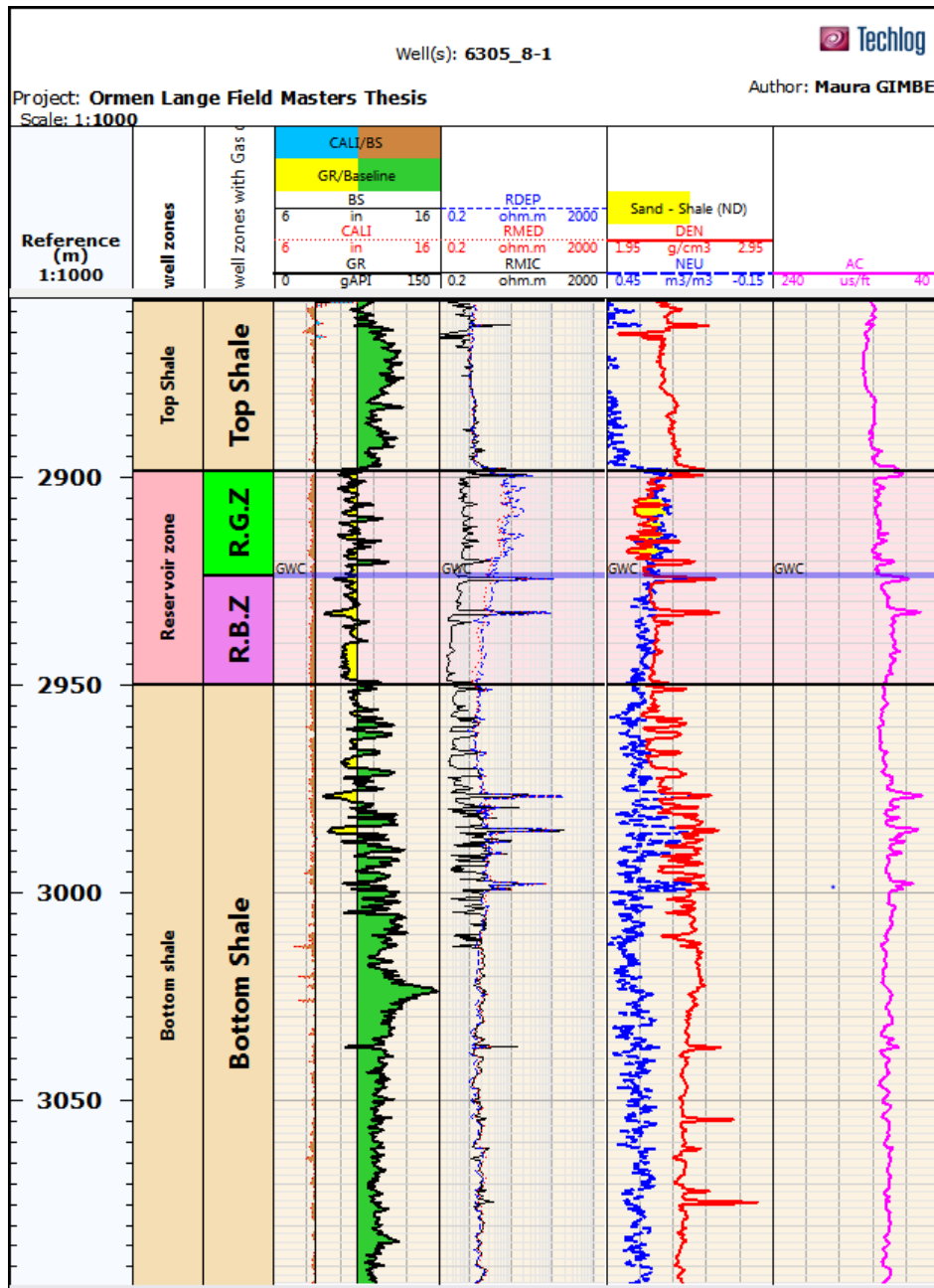


Figure 23: Well zone description for well 6305\_8-1

### 5.3 Vertical and lateral Variability

The lateral variations of facies and petrophysical properties of sandstone can be seen by correlations between the wells (Figure 25). The correlation of existing wells reveals in general lateral thickness variations within the reservoir interval at a level below, probably with exception of 6305/8-1 to 6305/5-1 where there is gentle thinning trend from thickening interval variation. There is a variation on reservoir patterns and evidence for compensating lateral changes between the wells between 6305/7-1, 6305/8-1 and 6305/5-1, commonly this happens in lowstand patterns. A relative change in facies can be seen in the correlation section showing a certain lateral and vertical continuity change in the well facies.

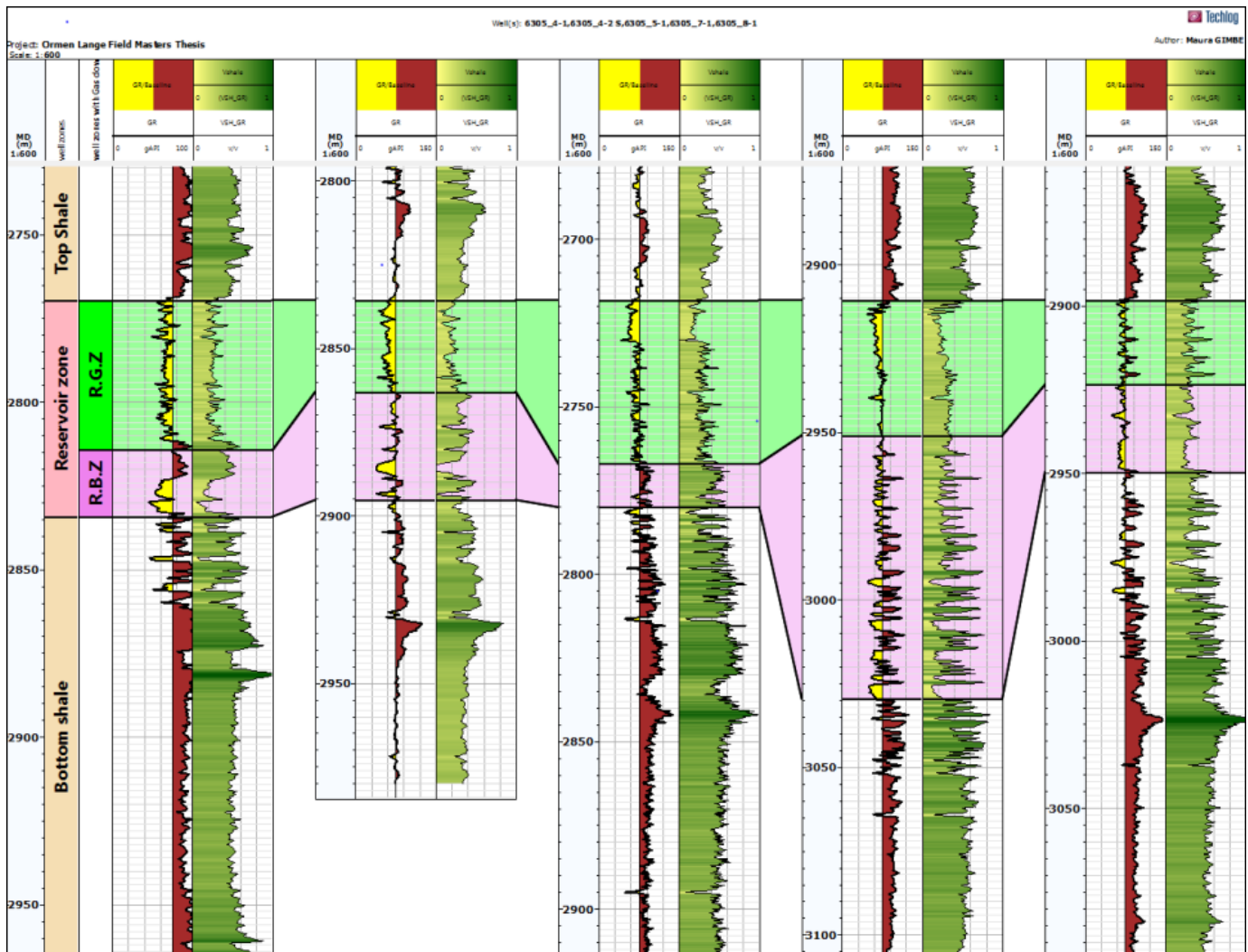


Figure 24: Well correlation for the 5 given wells at reservoir level

### Assumptions:

- ❖ It is assumed that the entire reservoirs are homogeneous
- ❖ The reservoirs of the five wells are divided into layers of equal thickness and are located roughly at the same depth interval.

### 5.4 Pre-computation

The result of bad hole computation indicated flags in some non-reservoir zones meaning possibly bad hole condition, but overall most of the reservoir zones show no warning of bad well conditions that may affect the quality of the reservoir measurements. The borehole computation showed a normal gradient of temperature around the wellbore.

### 5.5 Petrophysical Properties computation

It is important to identify properly the lithology and the reservoir to allow an accurate petrophysical calculation of porosity, water saturation and permeability. Therefore, in this section it was possible to discriminate and understand the reservoir zone.

Figure 26 displays shale volume ( $V_{shale}$ ), total porosity ( $PHIT$ ), effective porosity ( $PHIE$ ), permeability ( $Permeability\ coates$ ), water saturation ( $SWT$ ), gas saturation ( $S_{gi}$ ), rock, reservoir and pay flags. The reservoir is between 2769 to 2814m, it presents partially a clean and thick sand reservoir with 85% gas saturation average. The presence of low clay content seems to affect insignificantly the effective porosity and permeability values. Therefore, analyzing the average effective porosity (27%) and permeability of around 73-100mD, is concluded that this well presents a clean reservoir with a good permeability. The reservoir thickness matches with the pay zones.

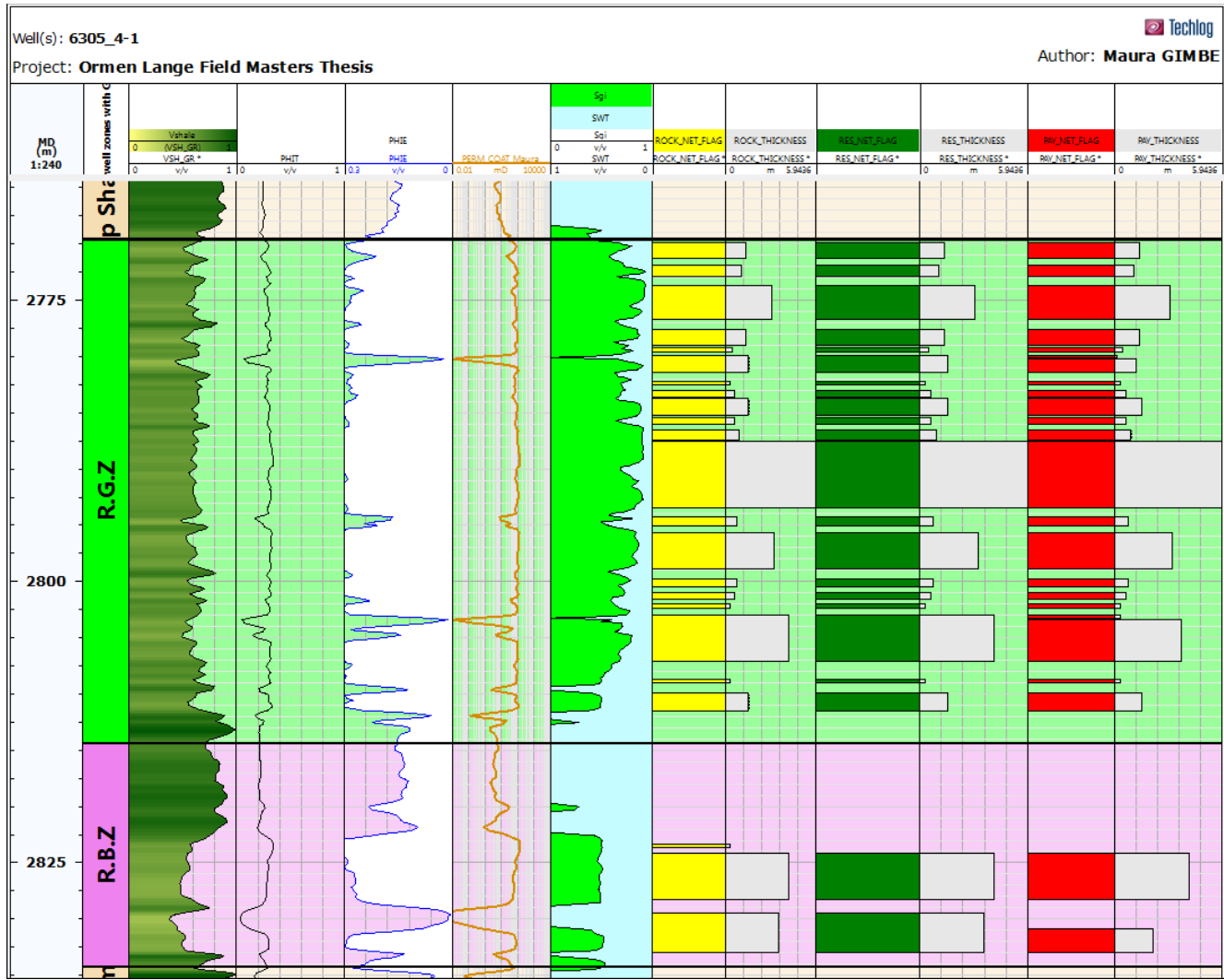


Figure 25: Petrophysical properties for well 6305\_4-1

Figure 27 displays shale volume ( $V_{shale}$ ), total porosity ( $PHIT$ ), effective porosity ( $PHIE$ ), permeability ( $Permeability\ coat$ ), water saturation ( $SWT$ ), gas saturation ( $S_{gi}$ ), rock, reservoir and pay flags. The reservoir is between of 2835 to 2862m, it presents partially a clean sand reservoir with 45% gas saturation average. The presence of shale layer mask the effective porosity, by filling up the porous as a consequence, decreasing the hydrocarbon accommodation space. Therefore, analyzing the average effective porosity (26%) and permeability of around 15-36 mD, then is concluded that this well presents a partially clean reservoir with good permeability. The pay zones do not match with the reservoir, showing a few thin pay intervals.

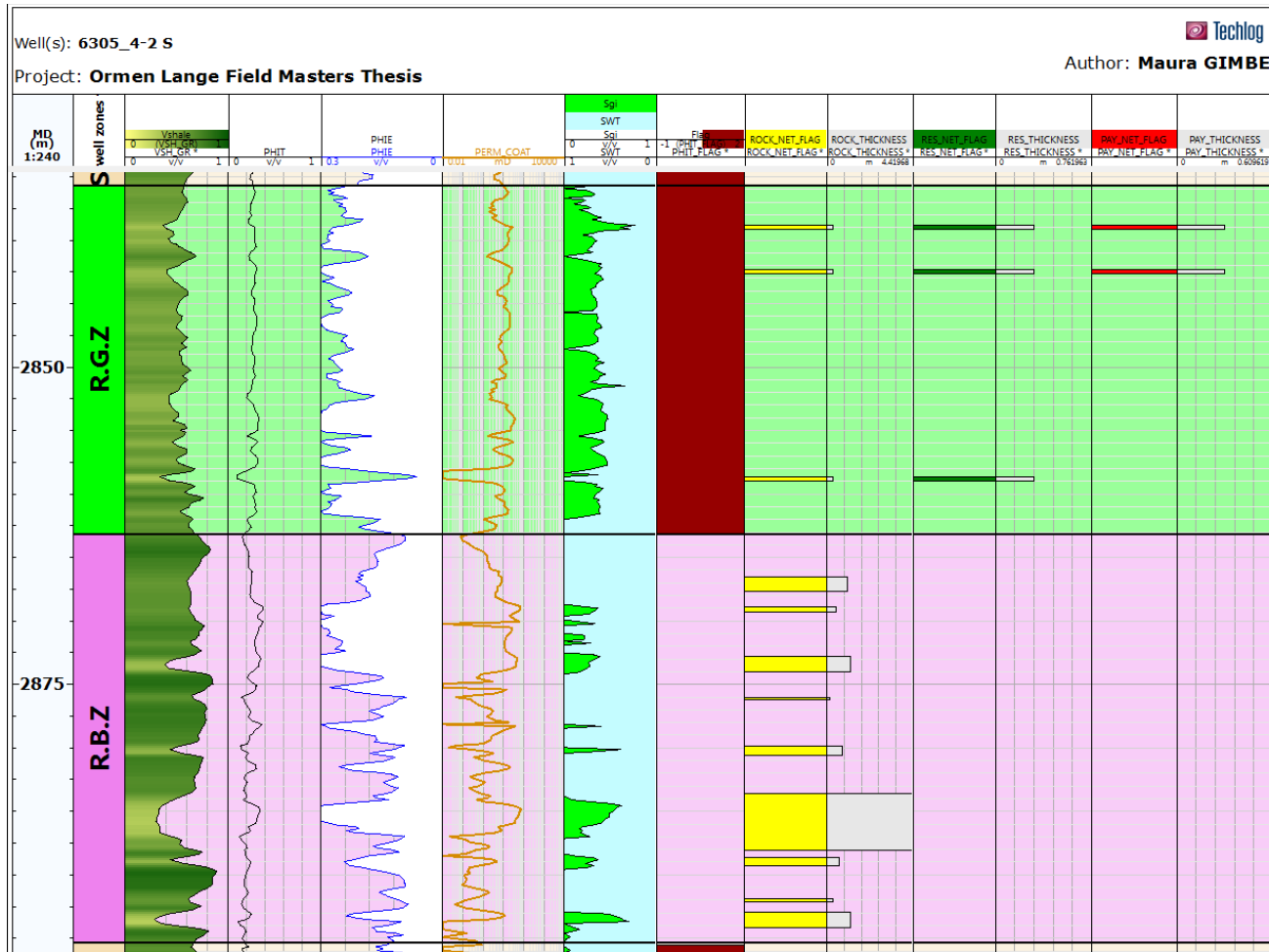


Figure 26: Petrophysical properties for well 6305\_4-2S

Figure 29 displays shale volume ( $V_{shale}$ ), total porosity ( $PHIT$ ), effective porosity ( $PHIE$ ), permeability ( $permeability\ coat$ ), water saturation ( $SWT$ ), gas saturation ( $S_{gi}$ ), rock, reservoir and pay flags. The reservoir is between of 2717 to 2766m, it presents partially a clean and thick sand reservoir with 83% gas saturation average. The presence of clay content seems to affect significantly the effective porosity and permeability values. Therefore, analyzing the average effective porosity (30%) and permeability of around 92-135mD, is concluded that this well presents a partially clean reservoir with a good permeability. The reservoir thickness matches with the pay zones.



Figure 27: Petrophysical properties for well 6305\_5-1

Figure 30 displays shale volume ( $V_{shale}$ ), total porosity ( $PHIT$ ), effective porosity ( $PHIE$ ), permeability ( $permeability\ coat$ ), water saturation ( $SWT$ ), gas saturation ( $Sg$ ), rock, reservoir and pay flags. The reservoir is between 2909 to 2950m, it presents partially a clean and thick sand reservoir with around 60-85% gas saturation. The presence of shale content seems to affect significantly the effective porosity and permeability values. Therefore, analyzing the average effective porosity (24%) and permeability of around 43-75mD, is concluded that this well presents a partially clean reservoir with a very good permeability. The reservoirs thickness matches with the pay zones.

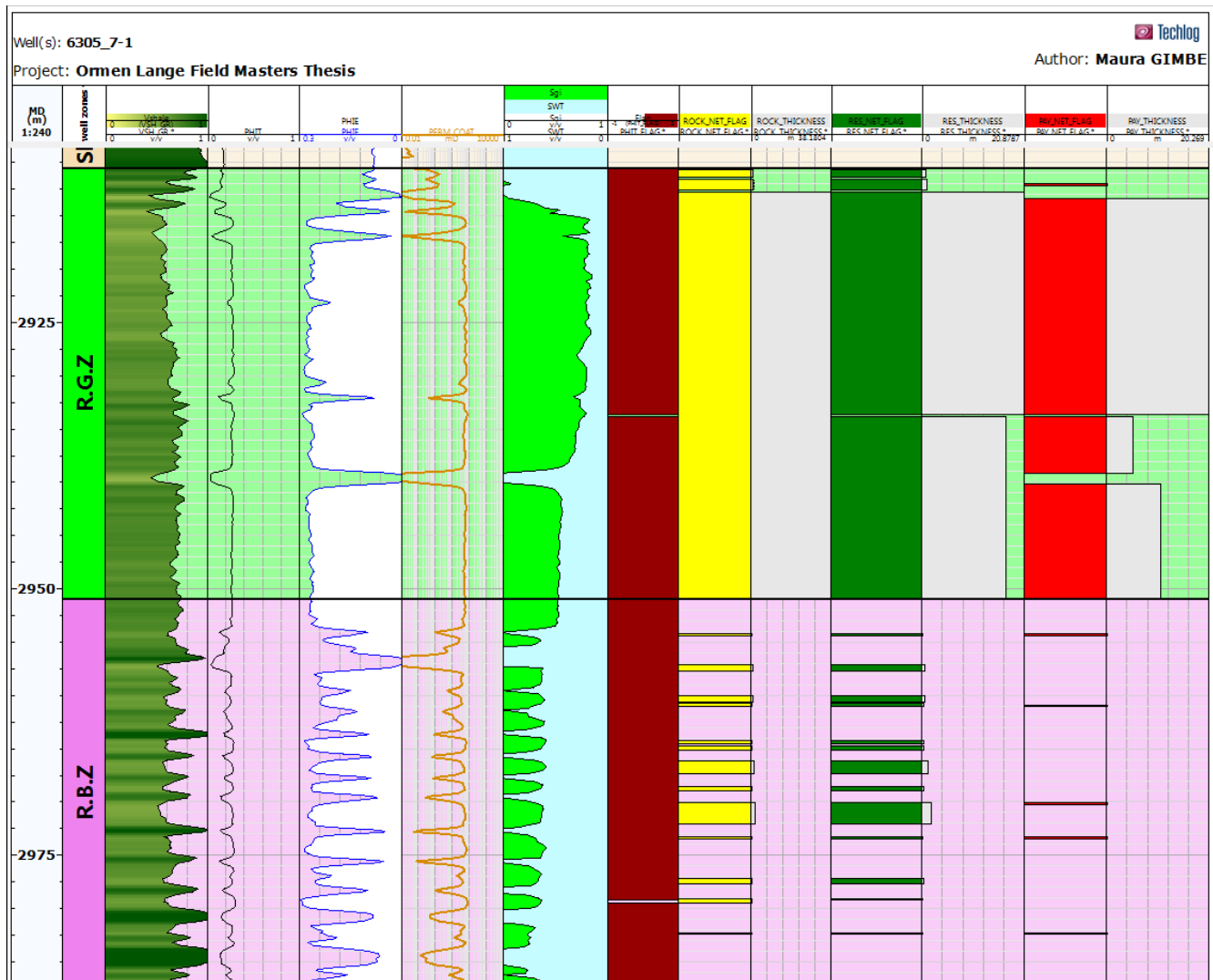


Figure 28: Petrophysical properties for well 6305\_7-1

Figure 31 displays shale volume ( $V_{shale}$ ), total porosity ( $PHIT$ ), effective porosity ( $PHIE$ ), permeability ( $Permeability\ coat$ ), water saturation ( $SWT$ ), gas saturation ( $S_{gi}$ ), rock, reservoir and pay flags. The reservoir is between 2897 to 2923m, it presents partially a clean and thick sand reservoir with 65% gas saturation average. The presence of shale content seems to affect significantly the effective porosity and permeability values. Therefore, analyzing the average effective porosity (24%) and permeability of around 59-120mD, is concluded that this well presents a partially clean reservoir with a good permeability. The reservoir thickness matches with the pay zones.



Figure 29: Petrophysical properties for well 6305\_8-1

### 5.6 Permeability uncertainty analysis

The results of permeability uncertainty analysis for the Ormen Lange field, applying sensitivity analysis and tornado plot generation, allowed to compare the relative weight of the variables on the computation. Therefore, in all the wells effective porosity affects the permeability computation more than the other variables as shown in Figures 32, 33, 34, 35, 36, the weight of the effective porosity on the Tornado plot was seen as the largest bar, the second was the irreducible water saturation and Coates permeability coefficient was the lesser. The Tornado plot analysis also shows a positive correlation between the effective porosity and the computed permeability while the irreducible water saturation has a negative correlation with the permeability. Permeability is not sensitive to total porosity.

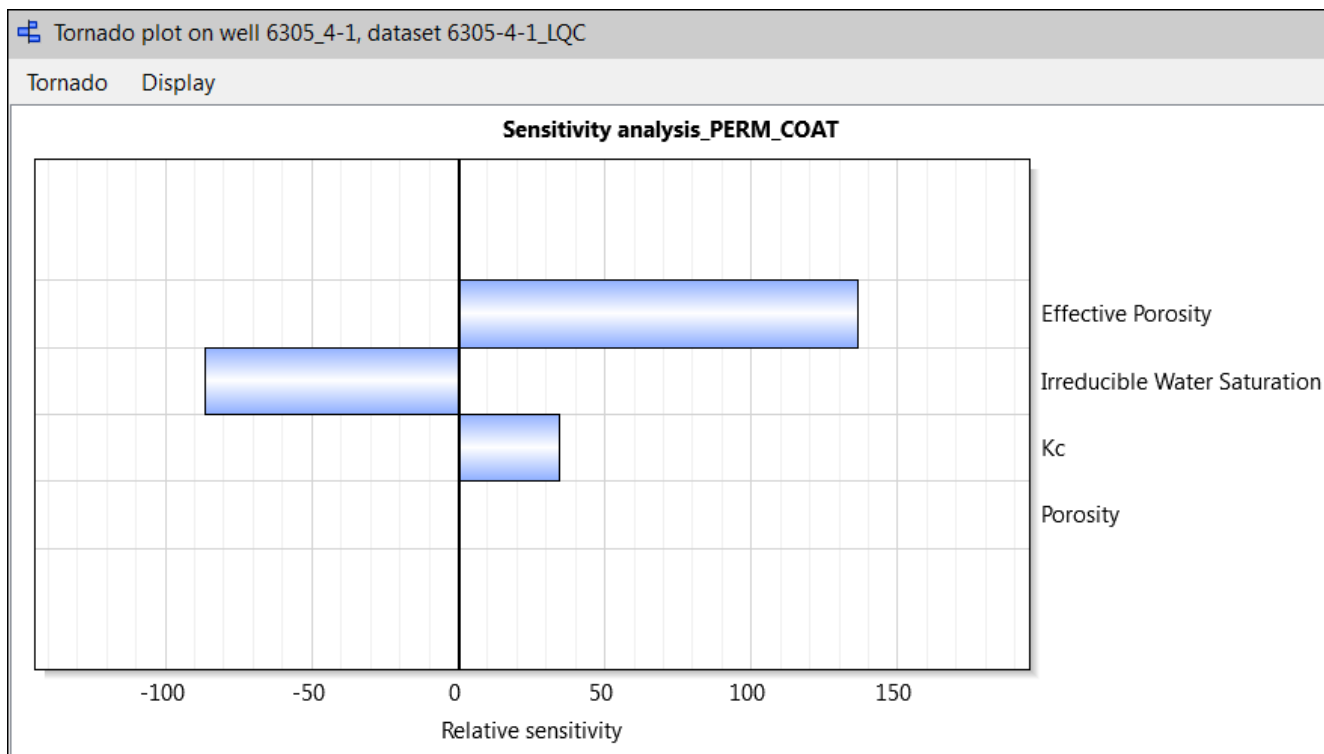


Figure 30: Sensitivity analysis for well 6305\_4-1

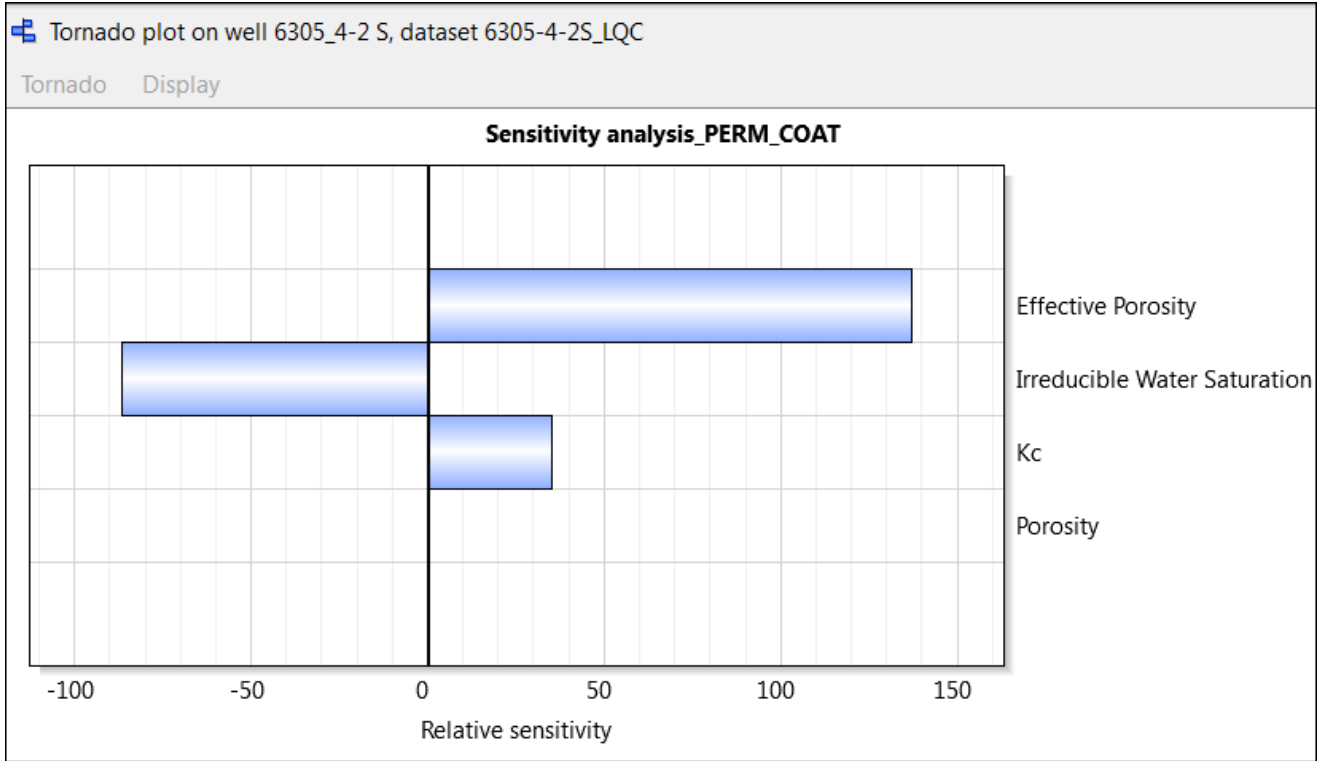


Figure 31: Sensitivity analysis for well 6305\_4-2S

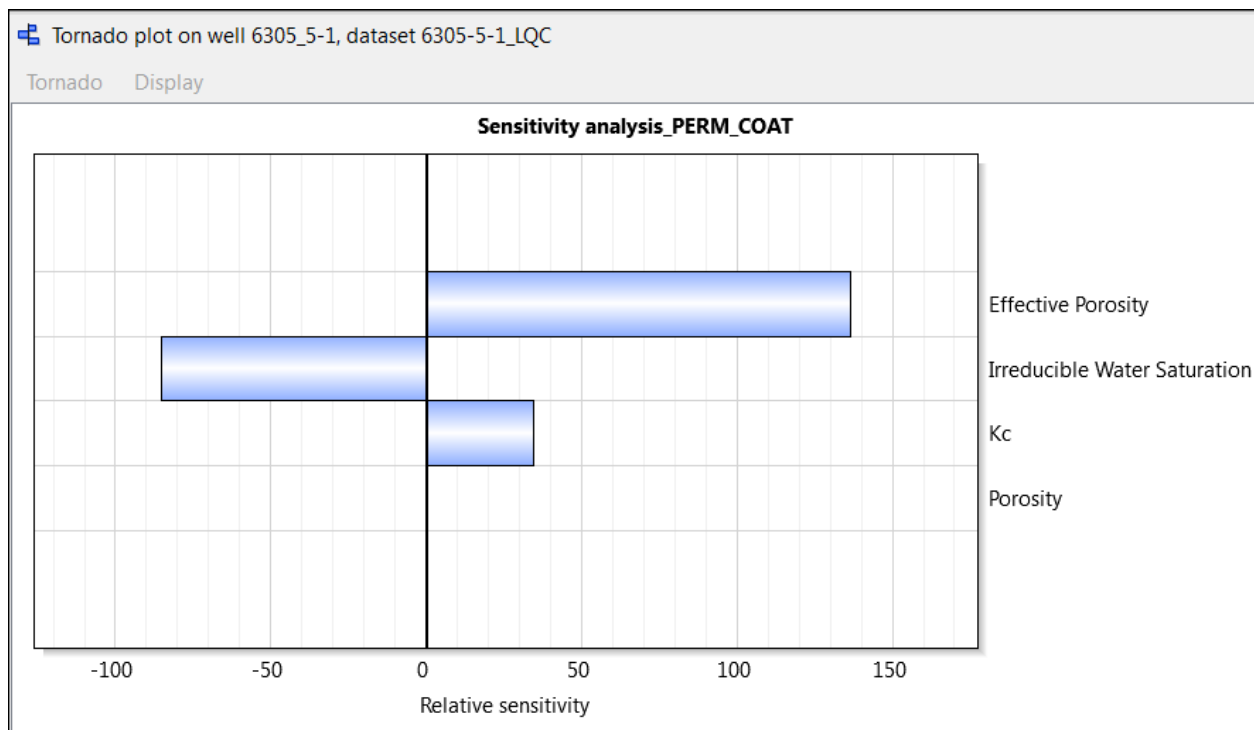


Figure 32: Sensitivity analysis for well 6305\_5-1

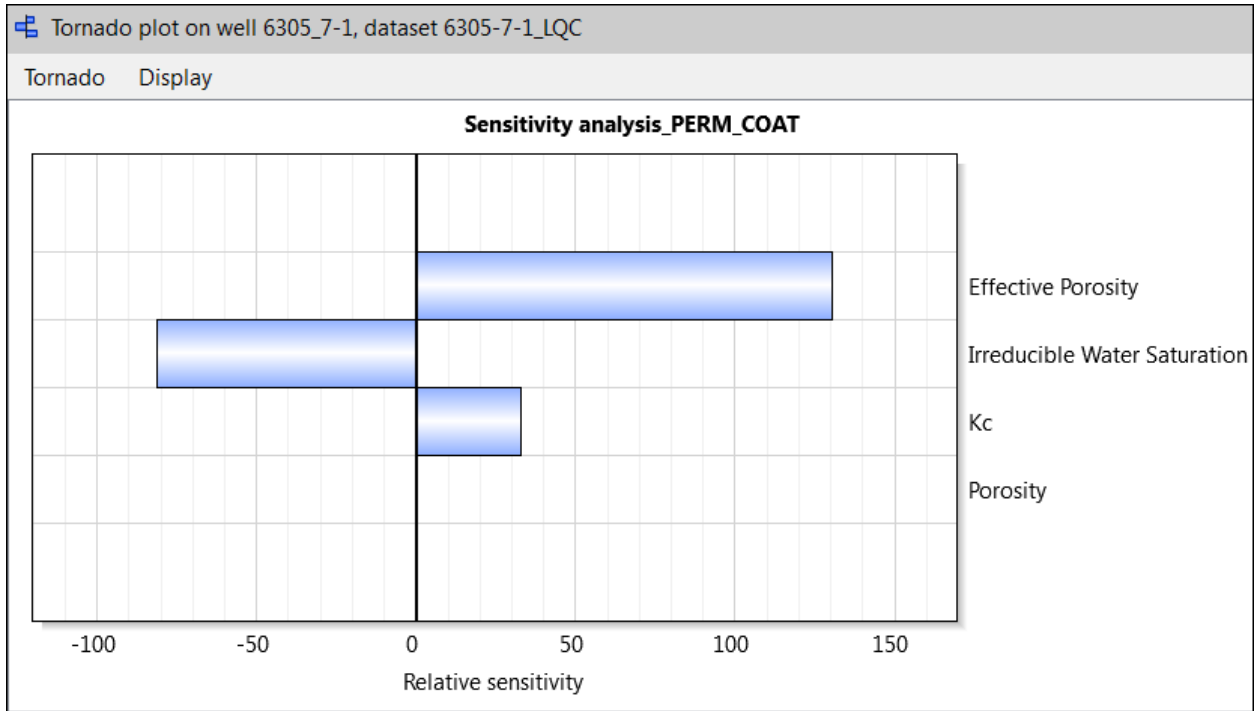


Figure 33: Sensitivity analysis for well 6305\_7-1

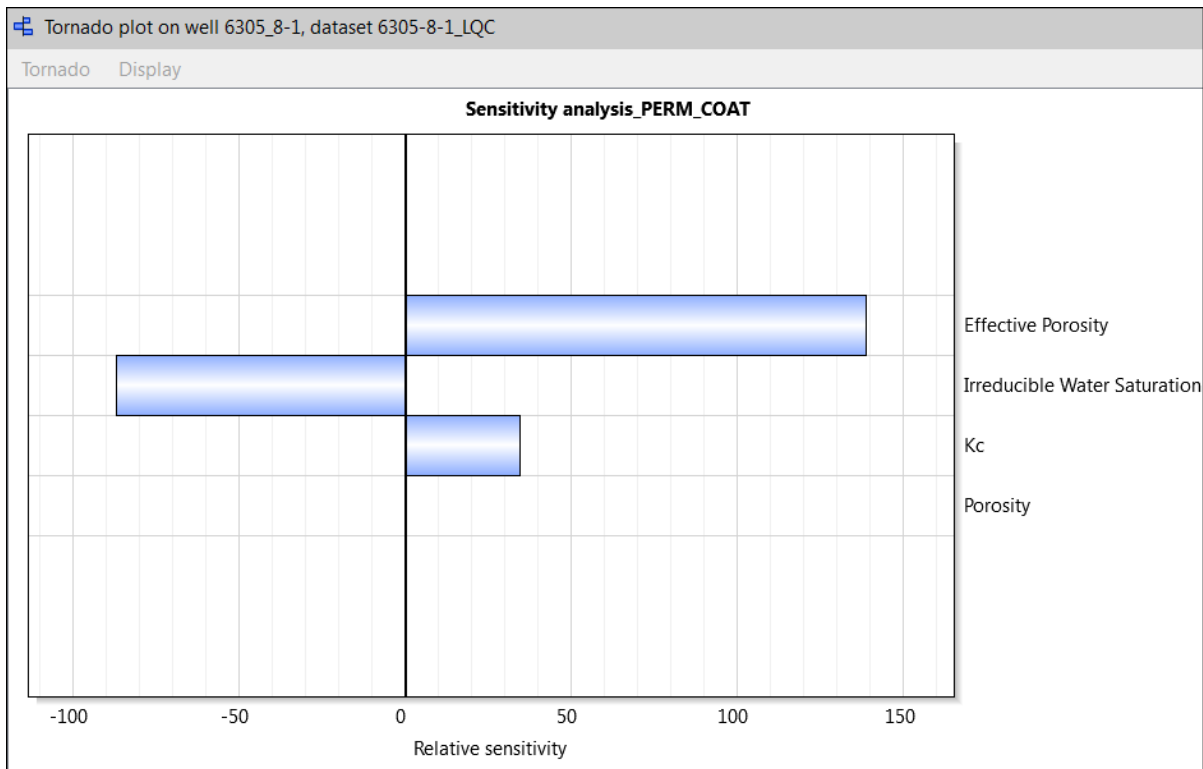


Figure 34: Sensitivity analysis for well 6305\_8-1

### 5.7 Porosity and permeability relationship on reservoir Zone

In general by plotting porosity values against permeability values showed strong linear relationship between the two variables of the reservoir indicating that Ormen Lange field reservoir are permeable. It should be noted that the shale presence influenced in on the permeability decreasing.

By plotting the effective porosity against permeability, it noticed that both curves increase simultaneously that possibly confirms the reservoir depositional environment as a turbidite fan (Figure 37). The regression line (red line) analyses of the wells 6305\_4-1, 6305\_7-1, 6305\_8-1 are probably located closer to proximal fan zone, as the points overlay the regression line. However, the wells 6305\_4-2S, 6305\_5-1 are probably located in the distal fan zone as the points are significantly away from regression line. The two wells are possible located on the distal part of turbidite fan.

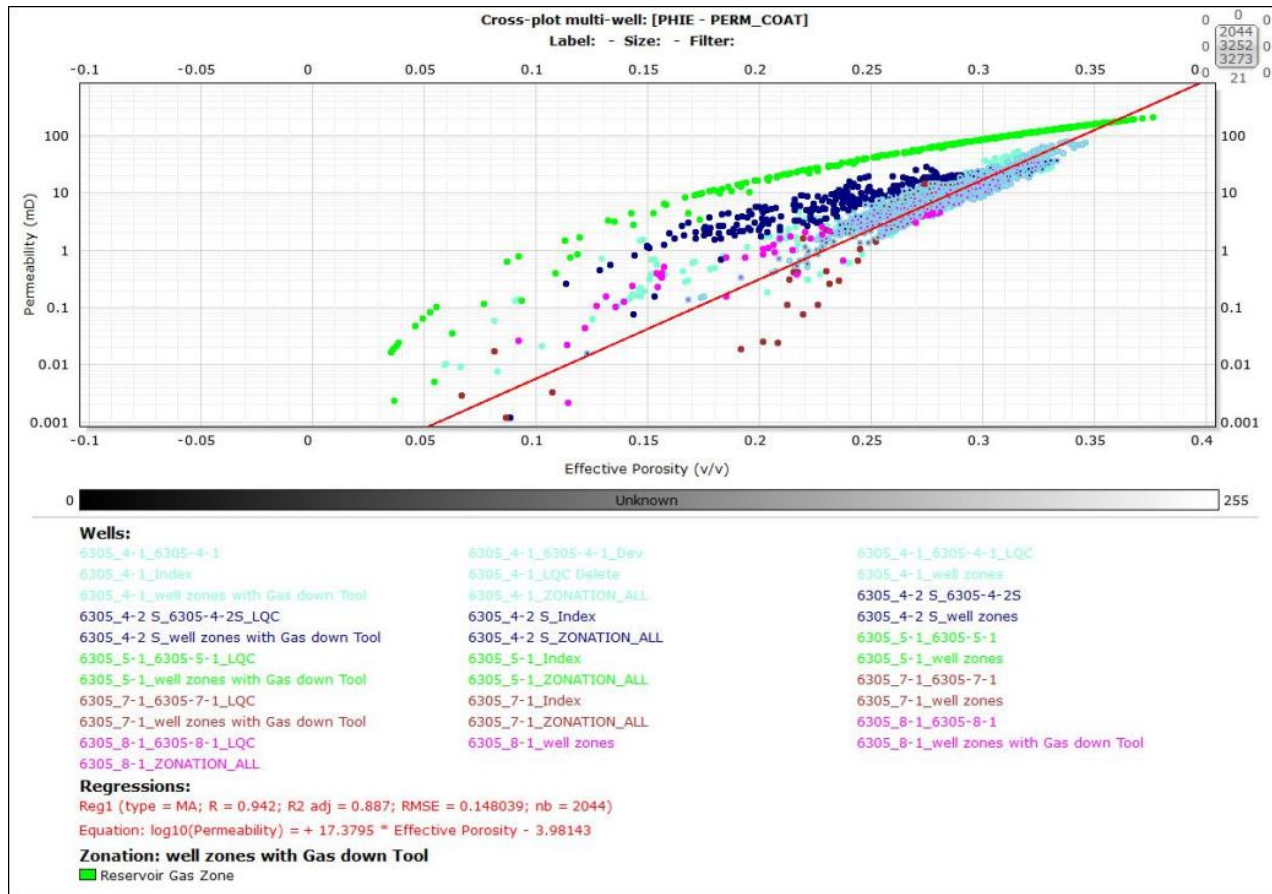


Figure 35: Cross plot Multi-well (PHIE vs PERM Coates)

## 5.7 Hydrocarbon volume Calculation

The STGOIP in Ormen Lange field was calculated following the steps:

- 1- Calculation of average net productive thickness of all the five wells
- 2- Calculation of average effective porosity of all the five wells
- 3- Calculation of the average saturation of all the five wells
- 4- Calculation of Initial gas saturated in the solution
- 5- Calculation of bulk reservoir volume
- 6- Calculation of formation volume factor for gas at initial conditions
- 7- Calculation of stock tank gas initial in place

### Given data:

$A = 345 \text{ km}^2 = 85253 \text{ acre}$ ,  $P = 289 \text{ bar} \approx 4192 \text{ psi}$ ,  $T = 93^\circ\text{C} = 200^\circ\text{F}$ ,

$T_{sc} = 15^\circ\text{C} = 59^\circ\text{F}$ ,  $Z = 0.8$

### Step 1

$$h_{4-1} = 45 \text{ ft}$$

$$h_{4-2} = 27 \text{ ft}$$

$$h_{5-1} = 49 \text{ ft}$$

$$h_{7-1} = 41 \text{ ft}$$

$$h_{8-1} = 26 \text{ ft}$$

$$h_{AV} = 37.6 \text{ ft}$$

### Step 2

$$\phi_{4-1} = 0.27$$

$$\phi_{4-2} = 0.26$$

$$\phi_{5-1} = 0.30$$

$$\phi_{7-1} = 0.24$$

$$\phi_{8-1} = 0.24$$

$$\phi_{AV} = 0.26$$

**Step 3**

$$S_{w\ 4-1} = 0.31$$

$$S_{w\ 4-2} = 0.67$$

$$S_{w\ 5-1} = 0.51$$

$$S_{w\ 7-1} = 0.47$$

$$S_{w\ 8-1} = 0.42$$

$$S_{w\ AV} = 0.48$$

**Step 4**

$$S_{gi} = (1 - S_w) = 1 - 0.48 = 0.52$$

**Step 5**

$$V_b = 43560 * A * h = 43560 * 85253 * 37.6 = 136.632 \text{ MMM } ft^3$$

**Step 6**

$$B_{gi} = \frac{P_{SC} * ZT}{T_{SC} * P} = \frac{14.7 * 0.8 * 200}{59 * 4190.5} = 0.00951 \frac{Ft^3}{SCF}$$

**Step 7**

$$STGOIP = \frac{136.632 * 10^9 * 0.26 * 0.52}{0.00951} = 1985.09 \text{ MMM } SCF$$

The hydrocarbon volume result of the reservoir is 1985.09 MMM SCF. In spite of some uncertainties mentioned above, this result is not far away from the one found in the research.

## CHAPTER 6- DISCUSSION

The data limitation such as PEF curve and Sonic became at certain time a barrier when it comes to choose the method to compute the effective porosity by Neutron-density/ PEF/ sonic using Techlog. Hence, it was used Neutron-density instead of PEF/Sonic. Likewise, the estimation of stock tank gas original in place (STGOIP) was an issue due to the difficulty to get the real area of the reservoir (A). Therefore, the area used was taken from literature reviewed in instead of seismic.

The calculated permeability based on Coates method presented some uncertainties. Therefore, the best way to ensure the reliability of permeability values is to compare this permeability with the one from core experiments (core permeability) and porosity and permeability relationship should be better explained. But in this work, it was not possible to do such comparison due lack of core data.

The wells 6350\_4-1, 6350\_5-1, 6350\_7-1, 6350\_8-1, presents slightly high permeability that ranged from 45-120 mD. Notwithstanding that, it doesn't discard the possibility of the reservoir to be affected by interbedded shale as show the cross-plots Neutron Porosity versus Bulk Density. This permeability values are still good for gas reservoir to be productive, taking into account the mobility and the very low gas viscosity it is just needed a large pressure differential to flow from very low permeability and low porosity rock interval into higher permeability conduit and to be the productive wellbore.

## CHAPTER 7- CONCLUSION

The formation evaluation done on Ormen Lange field enabled to come up with the following conclusions:

- ❖ Both log interpretations and Neutron-Density cross-plots confirmed that the reservoir consists of sand mixed with shale lithology. However, the cross-plot snapshot shows some dispersed points in the limestone field.
- ❖ By using the well log information it was possible to do well correlation and understand the continuity and variability of the facies on this field. It is possible to conclude that there is lateral and vertical continuity of facies between the wells.
- ❖ The average porosity and gas saturation of the reservoirs was about 0.26 and 0.52 respectively. While permeability values ranged from 45, to 135 mD indicating a very good reservoir quality.
- ❖ The estimated value of stock tank gas original in place (STGOIP) is still uncertainty due to the difficulty to get the real area of the reservoir (A).

## REFERENCES

- Adams, S.J., 2005. Quantifying Petrophysical Uncertainties. SPE 93125, presented at the 2005 Asia Pacific Oil & Gas Conference and Exhibition held in Jakarta, Indonesia, 5-7 April, 1- 6.
- Amaefule, J.O et al, 1989. Stochastic Approach to Computation of Uncertainties in Petrophysical Parameters. Society of Core Analysts, Paper No. SCA-8907.
- Archie, G.E., 1950. Introduction to Petrophysics of Reservoir Rocks. AAPG, Houston, Texas, 34 (5), 943-961.
- Ballin, P. R., Aziz, K., Journel, A. G., 1993. Quantifying the impact of geological uncertainty on reservoir performing forecast. Symposium on Reservoir Simulation, SPE 25238, New Orleans, Louisiana, February, 45-57.
- Bilgesu, H.I., et al., 1993. Formation Evaluation Using Core well log and initial Production data.SPE 26938, presented at the Eastern Regional Conference & Exhibition held in Pittsburgh, PA, U.S.A., 2-4 November, 437-444
- Bjerkreim, B., et al., 2007. Ormen Lange subsea compression Pilot.OTC 18969, presented at the Offshore Technology Conference held in Houston, Texas, U.S.A, 30 April-3 May, 1-11.
- Bouma, A. H., 1962. Sedimentology of some flysch Deposits. Elsevier, Amsterdam, New York
- Bouma, A. H., 2004. Key control on the characteristics of turbidite systems. Geological Society, London, 222, 9-22.
- Coates, G.R and Dumanoir, J. L., 1974. A New Approach to Improved Log-Derived Permeability. The Log Analyst, 8-17.
- Coope, D.F., Yearsley, E.N., 1986. Formation Evaluation Using EWR logs. SPE 14062, presented at the SPE International Meeting on Petroleum Engineering held in Beijing, China, 17-20 March, 415-425.
- Doré, A.G., Lundin, E.R (1996). Cenozoic Compressional structures on the NE Atlantic margin; nature, origin and potential significance for hydrocarbourn exploration. Petroleum Geoscience, 2, 299-311.
- Dullien, F. A. L, 1979: Porous Media, Fluid Transport and Pore Structure.
- Eirik, A.B., Per, A. K., 2004. Uncertainty, Risk and Decision Management on the Ormen Lange Gas Field Offshore Norway. Search and Discovery Article # 40112, presented at the AAPG International Conference, Barcelona, Spain, 21-24 September, 1-11.

Fugelli, E.M.G., et al., 2005, Screening for deep marine reservoir in frontier basins: Prt 1- Examples from offshore mid – Norway: AAPG Bulletin, 89(7), 853- 882.

Glover, P., 2011. Introduction to Petrophysics and Formation Evaluation. MSc Course Note. Available online at [http://homepages.see.leeds.ac.uk/~earpwig/PG\\_EN/CD%20Contents/GGL-66565%20Petrophysics%20English/Chapter%201.PDF](http://homepages.see.leeds.ac.uk/~earpwig/PG_EN/CD%20Contents/GGL-66565%20Petrophysics%20English/Chapter%201.PDF)

Grana, D., Pirrone, M., Mukerji, K., 2012. Quantitative log interpretation and uncertainty propagation of petrophysical properties and facies classification from rock-physics modeling and formation evaluation analysis. Geophysics 77(3).

Gregersen, S.E., 2014. Wet Gas Metering Challenges in Deep Water Field- The Shell Ormen Lange Experience.

Haddad, S., Cribbs, M., Sagar, R., Tang, Y., Viro, E., Castelijn, K., 2001. Integrating Permeabilities from NMR, Formation Tester, Well Test and Core Data. SPE 71722-MS, presented in SPE Annual Technical Conference and Exhibition, New Orleans, Louisiana, 30 September-3 October.

Hilchie, D. W., 1990. Reservoir Description Using Well Logs. JPT 1990, 35-41.

Jimmy, E., 2006. Ormen Lange Well Delivery. Mining Institute of Scotland, BP, Aberdeen, 8 November, 1-54.

Kapadia, S. P., and Menzie, D. E., 1985. Determination of Permeability Variation Factor V From Log Analysis. SPE 14402, presented at the Annual Technical Conference and Exhibition held in Las Vegas, NV, September, 22-25.

Link, 1982. Chapter 3- Permeability. Available online at <http://infohost.nmt.edu/~petro/faculty/Engler524/PET524-perm-1-ppt.pdf>

Liu, N., Oliver, D.S., 2003. Evaluation of Monte Carlo Methods for Assessing Uncertainty. SPE journal (2003) 8.

Lomas, S.A. and Joseph, P, 2004. Confined Turbidite Systems. Geological Society London, Special Publications, 222, 229-240.

Lowe, D.R., 1979, Sediment gravity flows: their classification and some problems of application to natural flows and deposits: SEPM Special Publication, 27, 75-82.

Lowe, D.R., 1982. Sediment gravity flows: II. Depositional models with special reference to the deposits of high-density turbidity currents: Journal of Sedimentary Petrology, 52, 279-297.

Ma, Y. Z., 2011. Uncertainty analysis in reservoir characterization and management: How much should we know about what we don't know?, in Ma, Y.Z. and La Pointe, P.R, eds., Uncertainty analysis and reservoir modeling: AAPG Memoir 96, 1-15.

Maschio, C., Schiozer, D.J., 2005. A methodology to quantify the impact of uncertainties in the history matching process and in the production forecast. SPE Annual Technical Conference and Exhibition, SPE 96613, Dallas, Texas, October, 10.

Möller, et al., 2004. A geological model for the Ormen Lange hydrocarbon reservoir. Norwegian Journal of Geology, 84(3), p169.

Pickering, K.T., Hiscott., R.N., Kenyon, N.H., Ricci Lucchi, F., and Smith, R.D.A(eds.), 1995. Atlas of Deep water Environments. Chapman et Hall, London, 1-10.

Pradyut, B., 1979. Formation Evaluation Based on Logging data. Geology & Reservoir Deptt. Available online at <http://petrofed.winwinhosting.net/upload/30May-01June11/7.pdf>

Riis, F.,1996. Quantification of Cenozoic vertical movements of Scandinavia by correlation of morphological surfaces with offshore data. Global Planetary Changes, 12, 331-357.

Schlumberger Limited, Log Interpretation Charts, (1989) Houston, Texas.

Schlumberger Oilfield Services, and Y. Tang, SPE, U. of Tulsa - SPE 63138.

Schlumberger Publication, 2013. Neutron Porosity Tools. [Unpublished Training course notes](#).

Shepherd, M., 2009. Deep-water marine reservoirs, in M. Shepherd, Oil field production geology: AAPG Memoir, 91, 295-300.

Storvoll et al., 2002. Porosity preservation in reservoir sandstones due to grain- coating illite: a study of the Jurassic garn formation from the Kristin and Lavrans fields offshore Mid- Norway. Marine and Petroleum Geology – MAR PETROL GEOL, 19 (9), 767-781.

Stow, D.A.V., 1980. Sequence of structures in fine-grained turbidites: Comparison of recent deep sea and ancient flysch sediments. Sediment Geology, 25, 23-42.

Sullivan, M.D., Jensen, G.N., Goulding, F.J., Jennette, D.C., and Stern, D., 2000. Architectural analysis of deep water outcrops: Implications for exploration and production of the Diana Sub-basin, western Gulf of Mexico. In: P. Weimer, R.M. Slatt, A.H. Bouma, and D.T. Lawrence, eds., Gulf Coast section, 1010-1032.

Theodoor, W.F., 2000. Small Rock Samples using Image Analysis Techniques. Technical University of Delft, 14 November, 1-193.

Thomas, E.C. 1992. 50th Anniversary of the Archie Equation: Archie Left More Than Just an Equation. The Log Analyst, 33(3), 199-205.

Timur, A., 1968. An Investigation of Permeability, Porosity, and Residual Water Saturation Relationship for Sandstone reservoir. The log Analyst journal, July- Aug, 8-17.

Tixier, M. P., 1949. Evaluation of Permeability from Electric log Resistivity Gradients. Oil & Gas Journal, 16 June, 113.

Weimer, P., Slatt, R.M., 1999. Turbidite systems, Part 1: Sequence and seismic stratigraphy: The Leading Edge, 18(4), 454–463.

Willian, M.R., et al., 2011. Uncertainty Analysis in well- log and Petrophysical Interpretations, in Y. Z. Ma and P. R. La Pointe, eds., Uncertainty analysis and reservoir modeling: AAPG Memoire 96, 17–28.

Wilson, A., et al., 2004. Ormen Lange – Flow Assurance Challenges. OTC 16555, presented at the Offshore Technology Conference held in Houston, Texas, U. S. A., 3-6 May 2004, 1-10.